Flux Emergence Workshop 2017
Budapest Hungary, June 15th 2015

Relative magnetic helicity as a diagnostic of solar eruptivity in flux emergence simulations (and others)

É. Pariat[1], J. Leake[2], G. Valori[3] , M. Linton[4],
F. Zuccarello[5], K. Dalmasse[6], K. Moraitis[1], L. Linan[1]

[1] LESIA, Observatoire de Paris, PSL*, CNRS, UPMC, Univ. D. Diderot, France
[2] NASA Goddard Space light Center, Greenbelt MD, USA
[3] MSSL, Univ. College London, UK
[4] Naval Research Laboratory, Washington DC, USA
[5] KU Leuven, Belgium
[6] NCAR, Boulder, CO, USA

Outline

- **Introduction: flare & eruption previsions**
- Flux emergence model: Leake et al. 2013 & 2014
- Eruptivity criterion analysis
  - Magnetic flux & energy-based quantities
  - Magnetic-helicity-based quantities
    - Relative magnetic helicity
    - Current-carrying magnetic helicity
- Other models & Conclusions

Efficiency of flares & eruptions forecasting

(Crown et al. 12)

- Multiplication of daily forecasts centers and methods: MET Office, SWPC, SIDC, …

- **Barnes et al. 2016**: comparison of a large number of forecasting methods with a common dataset:
  - **"[…], none of the methods achieves a particularly high skill score. […].Thus there is considerable room for improvement in flare forecasting."**

SUCCESS RATES AND SKILL SCORES FOR THE SAMPLE PARAMETERS

Parameter	Success Rate	Heidke Skill Score	Climatological Skill Score
No Flare	0.908	0.000	0.000
Φ_{tot}	0.922	0.153	0.197
E_e	0.916	0.081	0.231
R	0.922	0.144	0.242
B_{eff}	0.913	0.072	0.220

Table 4. Performance on All Data with Reference Forecast

Parameter/ Method	Statistical Method	C1.0+, 24 hr		M1.0+, 12 hr		M5.0+, 12 hr	
		ApSS	BSS	ApSS	BSS	ApSS	BSS
B_{eff}	Bayesian	0.12	0.06	0.00	0.03	0.00	0.02
ASAP	Machine	0.25	0.30	0.01	-0.01	0.00	-0.84
BBSO	Machine	0.08	0.10	0.03	0.06	0.00	-0.01
WL_{SG2}	Curve fitting	N/A	N/A	0.04	0.06	0.00	0.02
NWRA MAG 2-VAR	NPDA	0.24	0.32	0.04	0.13	0.00	0.06
$\log(\mathcal{R})$	NPDA	0.17	0.22	0.01	0.10	0.02	0.04
GCD	NPDA	0.02	0.07	0.00	0.03	0.00	0.02
NWRA MCT 2-VAR	NPDA	0.23	0.28	0.05	0.14	0.00	0.06
SMART2	CCNN	0.24	-0.12	0.01	-4.31	0.00	-11.2
Event Statistics, 10 prior	Bayesian	0.13	0.04	0.01	0.10	0.01	0.00
McIntosh	Poisson	0.15	0.07	0.00	-0.06	N/A	N/A

(Barnes et al 16)

Flares & eruptions forecasting approach

- **Prediction are not based on determinist approach but on an empirical one**:
- Correlations between:
  - Characteristics of an active region: McIntosh class, Mt Wilson magnetic class, PIL length, magnetic properties, …
  - Observed probability for a region with a given characteristic to flare

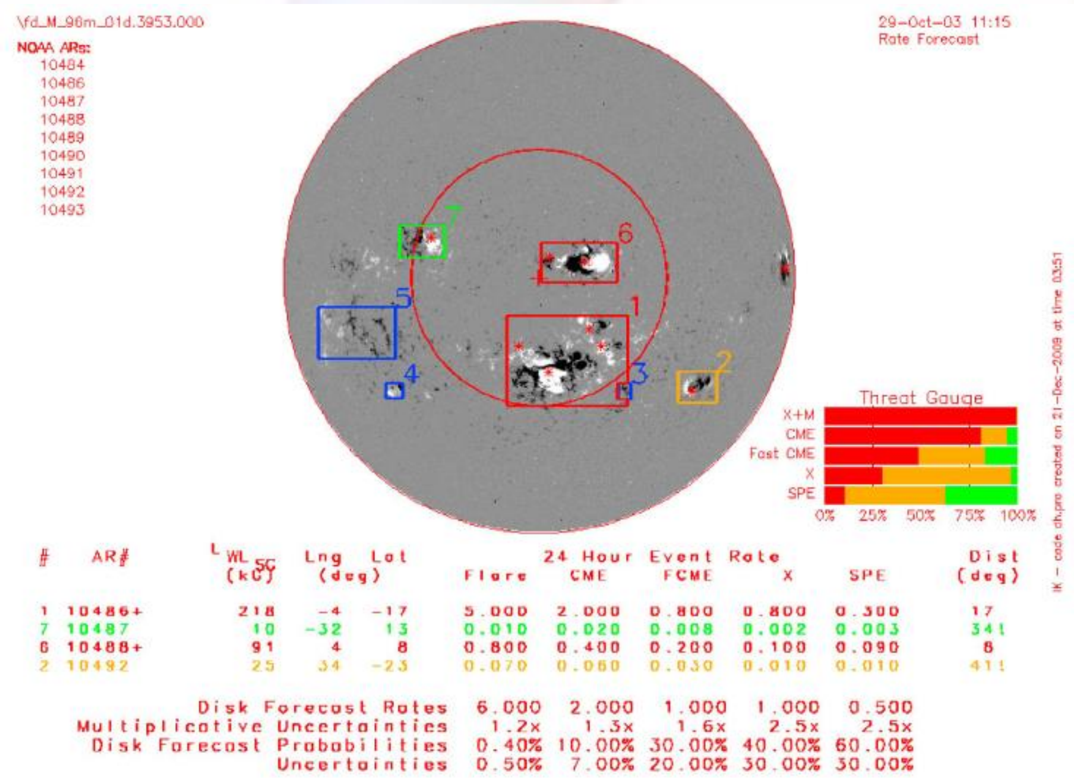

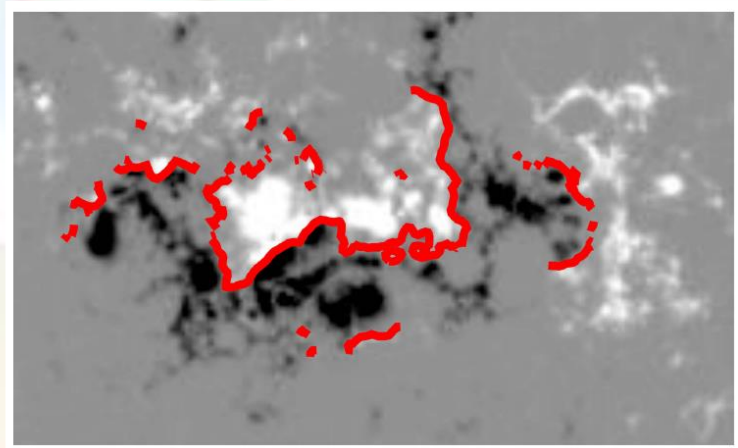

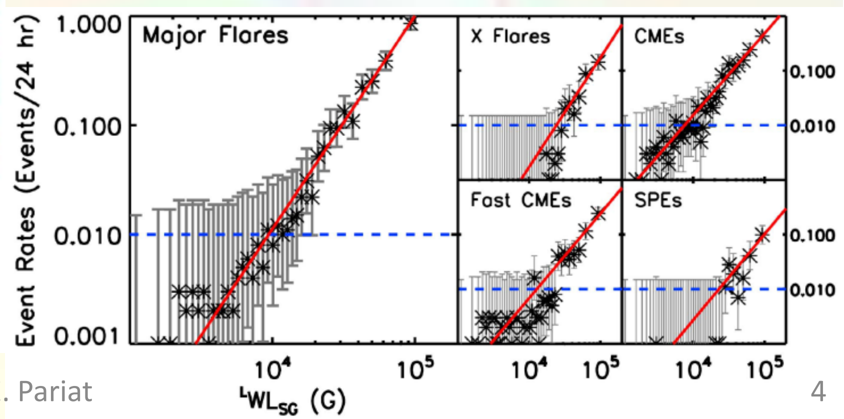

(Falconer et al. 11)

Flaring/eruptivity criterion

- Single criteria alone always gives very poor prediction
  - Combination of several criterion improves prediction.

- **➔ Prediction criterion are only based on necessary conditions for eruption**
  - e.g. based on the energy build-up of active region

- **No clear physical criterion of sufficient conditions for eruption trigger**

(Leka & Barnes 07)

TABLE 1
Parameters Used in the Discriminant Analysis

Description	Formula	Variable
Atmospheric Seeing		
Median of the granulation contrast	$s = \mathrm{median}(\Delta I)$	s
Distribution of Magnetic Fields		
Moments of vertical magnetic field	$B_z = \boldsymbol{B} \cdot \boldsymbol{e}_z$	$\mathcal{M}(B_z)$
Total unsigned flux	$\Phi_{\mathrm{tot}} = \sum \lvert B_z \rvert \, dA$	Φ_{tot}
Absolute value of the net flux	$\lvert \Phi_{\mathrm{net}} \rvert = \lvert \sum B_z \, dA \rvert$	$\lvert \Phi_{\mathrm{net}} \rvert$
Moments of horizontal magnetic field	$B_h = \left(B_x^2 + B_y^2\right)^{1/2}$	$\mathcal{M}(B_h)$
Distribution of Inclination Angle		
Moments of inclination angle	$\gamma = \tan^{-1}(B_z/B_h)$	$\mathcal{M}(\gamma)$
Distribution of the Magnitude of the Horizontal Gradients of the Magnetic Fields		
Moments of total field gradients	$\lvert \nabla_h B \rvert = \left[(\partial B/\partial x)^2 + (\partial B/\partial y)^2\right]^{1/2}$	$\mathcal{M}(\lvert \nabla_h B \rvert)$
Moments of vertical field gradients	$\lvert \nabla_h B_z \rvert = \left[(\partial B_z/\partial x)^2 + (\partial B_z/\partial y)^2\right]^{1/2}$	$\mathcal{M}(\lvert \nabla_h B_z \rvert)$
Moments of horizontal field gradients	$\lvert \nabla_h B_h \rvert = \left[(\partial B_h/\partial x)^2 + (\partial B_h/\partial y)^2\right]^{1/2}$	$\mathcal{M}(\lvert \nabla_h B_h \rvert)$
Distribution of Vertical Current Density		
Moments of vertical current density	$J_z = C(\partial B_y/\partial x - \partial B_x/\partial y)$	$\mathcal{M}(J_z)$
Total unsigned vertical current	$I_{\mathrm{tot}} = \sum \lvert J_z \rvert \, dA$	I_{tot}
Absolute value of the net vertical current	$\lvert I_{\mathrm{net}} \rvert = \lvert \sum J_z \, dA \rvert$	$\lvert I_{\mathrm{net}} \rvert$
Sum of absolute value of net currents in each polarity	$\lvert I^B_{\mathrm{net}} \rvert = \lvert \sum J_z(B_z > 0) \, dA \rvert + \lvert \sum J_z(B_z < 0) \, dA \rvert$	$\lvert I^B_{\mathrm{net}} \rvert$
Moments of vertical heterogeneity current density[a]	$J_z^h = C(b_y \partial B_x/\partial y - b_x \partial B_y/\partial x)$	$\mathcal{M}(J_z^h)$
Total unsigned vertical heterogeneity current	$I^h_{\mathrm{tot}} = \sum \lvert J_z^h \rvert \, dA$	I^h_{tot}
Absolute value of net vertical heterogeneity current	$\lvert I^h_{\mathrm{net}} \rvert = \lvert \sum J_z^h \, dA \rvert$	$\lvert I^h_{\mathrm{net}} \rvert$
Distribution of Twist Parameter		
Moments of twist parameter[b]	$\alpha = C J_z / B_z$	$\mathcal{M}(\alpha)$
Best-fit force-free twist parameter[b]	$\boldsymbol{B} = \alpha_{\mathrm{ff}} \nabla \times \boldsymbol{B}$	$\lvert \alpha_{\mathrm{ff}} \rvert$
Distribution of Current Helicity		
Moments of current helicity[c]	$h_c = C B_z (\partial B_y/\partial x - \partial B_x/\partial y)$	$\mathcal{M}(h_c)$
Total unsigned current helicity	$H_c^{\mathrm{tot}} = \sum \lvert h_c \rvert \, dA$	H_c^{tot}
Absolute value of net current helicity	$\lvert H_c^{\mathrm{net}} \rvert = \lvert \sum h_c \, dA \rvert$	$\lvert H_c^{\mathrm{net}} \rvert$
Distribution of Shear Angles		
Moments of 3D shear angle[d]	$\Psi = \cos^{-1}(\boldsymbol{B}^p \cdot \boldsymbol{B}^o / B^p B^o)$	$\mathcal{M}(\Psi)$
Area with shear $>\Psi_0$, $\Psi_0 = 45^\circ, 80^\circ$	$A(\Psi > \Psi_0) = \sum_{\Psi > \Psi_0} dA$	$A(\Psi > 45^\circ)$, $A(\Psi > 80^\circ)$
Moments of neutral line shear angle	$\Psi_{\mathrm{NL}} = \cos^{-1}(\boldsymbol{B}^p_{\mathrm{NL}} \cdot \boldsymbol{B}^o_{\mathrm{NL}} / B^p_{\mathrm{NL}} B^o_{\mathrm{NL}})$	$\mathcal{M}(\Psi_{\mathrm{NL}})$
Length of neutral line with shear $>\Psi_0$	$L(\Psi_{\mathrm{NL}} > \Psi_0) = \sum_{\Psi_{\mathrm{NL}} > \Psi_0} dL$	$L(\Psi_{\mathrm{NL}} > 45^\circ)$, $L(\Psi_{\mathrm{NL}} > 80^\circ)$
Moments of horizontal shear angle[e]	$\psi = \cos^{-1}(\boldsymbol{B}^p_h \cdot \boldsymbol{B}^o_h / B^p_h B^o_h)$	$\mathcal{M}(\psi)$
Area with horizontal shear $>\psi_0$	$A(\psi > \psi_0) = \sum_{\psi > \psi_0} dA$	$A(\psi > 45^\circ)$, $A(\psi > 80^\circ)$
Distribution of Photospheric Excess Magnetic Energy Density		
Moments of photospheric excess magnetic energy density[d]	$\rho_e = (\boldsymbol{B}^p - \boldsymbol{B}^o)^2 / 8\pi$	$\mathcal{M}(\rho_e)$
Total photospheric excess magnetic energy	$E_e = \sum \rho_e \, dA$	E_e

Eruptivity prediction & numerical modeling

- **Search for eruptivity criterion is almost exclusively based on observational datasets …**
- **… and barely benefits from the recent tremendous improvements in numerical modeling .**

- Useful numerical models must present several cases either eruptive or stable, ideally
  - > 2 cases
  - depending on few number of parameters

- **Kusano et al. 2012**: parametric analysis based on relative orientation of large scale sheared polarity and small scale

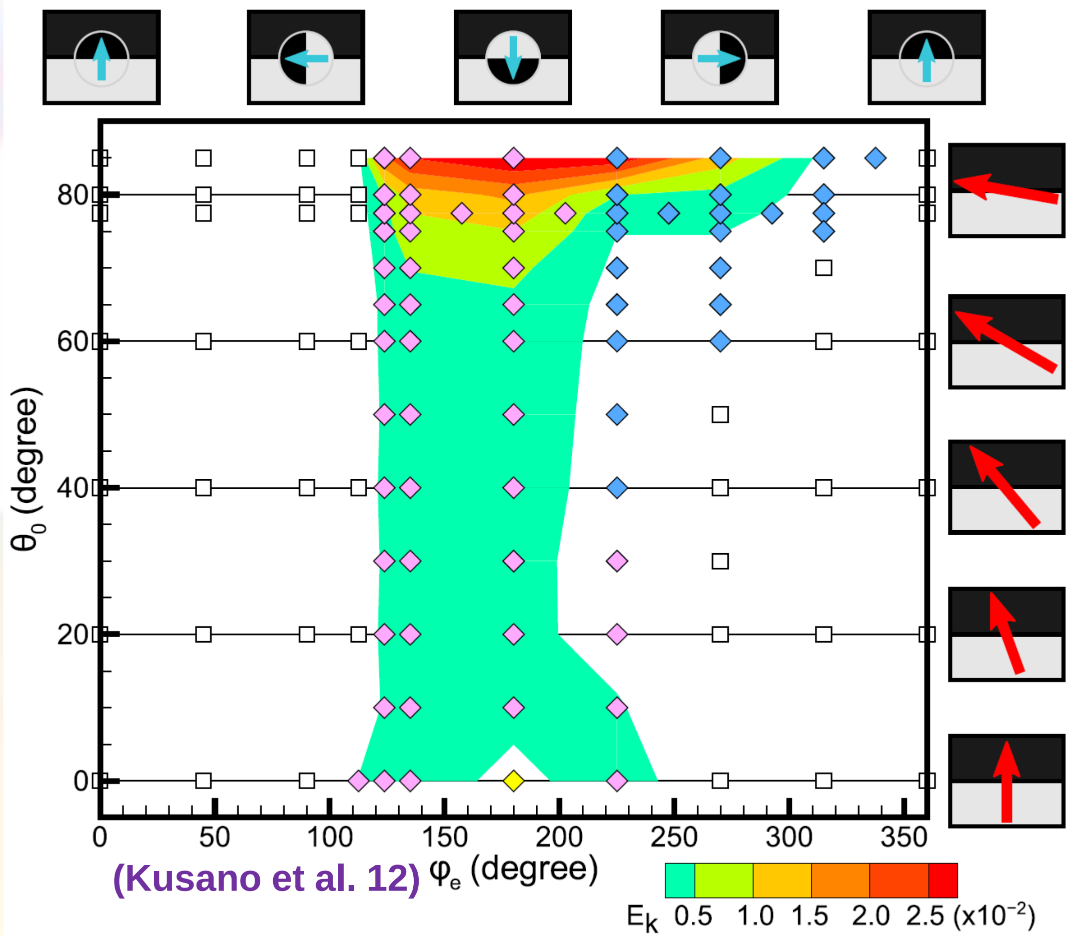

(Kusano et al. 12)

Motivations & Methodology

- **Goal: use flux emergence simulations to look for efficient eruptivity criterion**
  - **Leake et al. 2013 and Leake et al. 2014**:
    - **7 flux emergence simulations**
    - 3D visco-resistive MHD eq. solved with Lagrangian-remap code **(Arber et al. 2001)**
    - **lead to eruptive and non-eruptive cases**
    - **varying only an unique initial parameter**

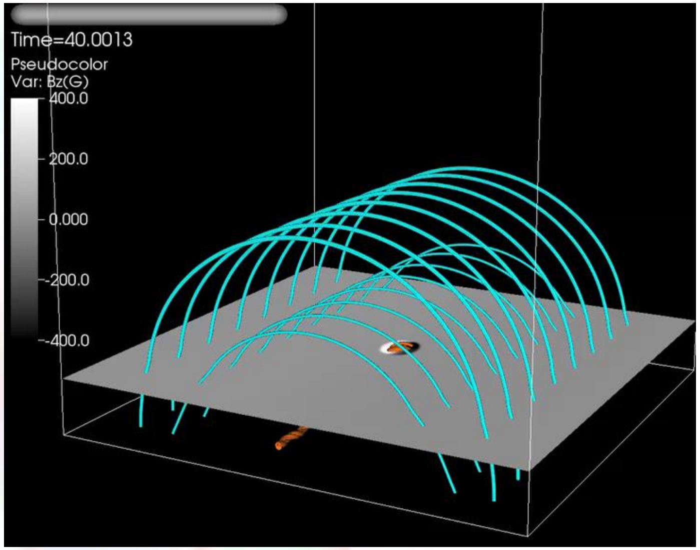

(Leake et al. 13, 14)

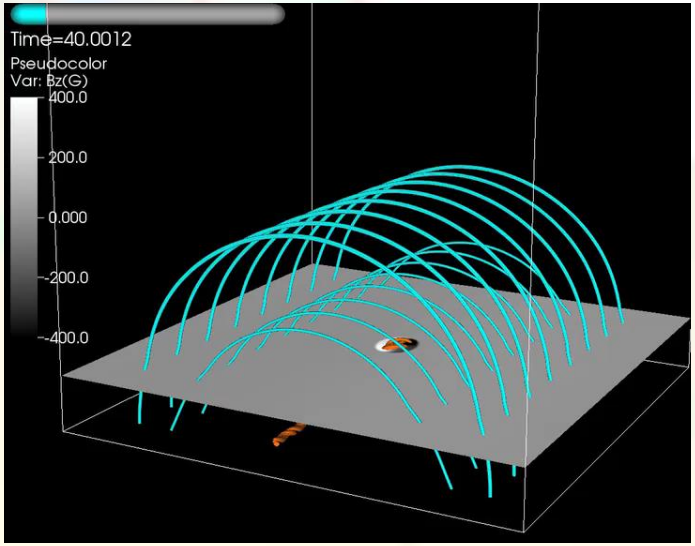

- Methodology: - extract part of the magnetic field,
  - compute different physical quantities,
  - search for the ones that discriminates between the eruptive and non-eruptive case
- **Guennou et al. 17**: **<u>2D photospheric mag. field</u>**
  - similarly to observed data
  - 99 physical quantities studied.
- **This talk: <u>3D coronal magnetic field B(z>0)</u>**

Outline

- Introduction: flare & eruption previsions
- **Flux emergence model: Leake et al. 2013 & 2014**
- Eruptivity criterion analysis
  - Magnetic flux & energy-based quantities
  - Magnetic-helicity-based quantities
    - Relative magnetic helicity
    - Current-carrying magnetic helicity
- Other models & Conclusions

Parametric flux emergence simulations

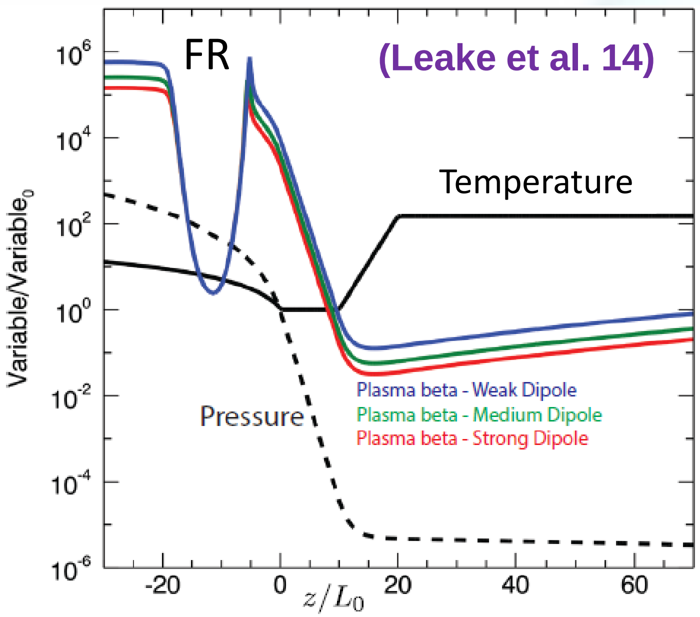

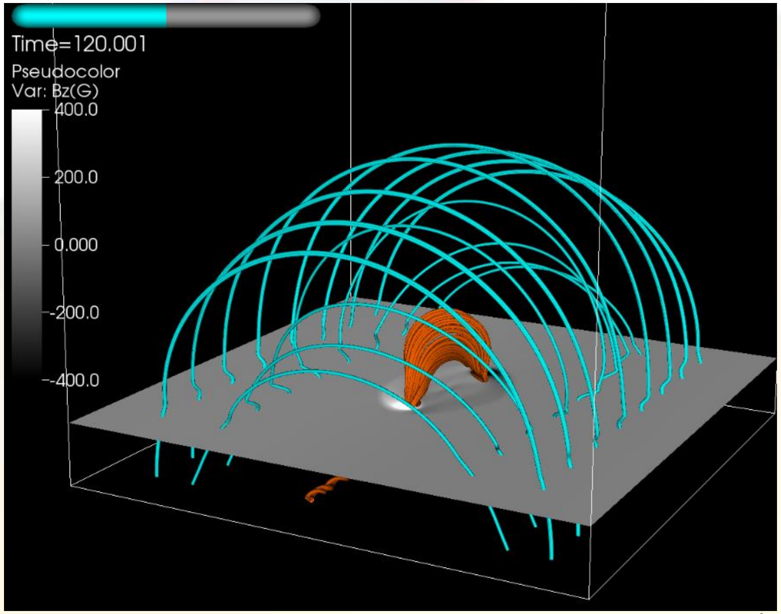

- Twisted FR emerge in coronal arcade field
- **Emerging twisted flux rope: identical in all cases**
- **Overlying arcade field: 1 param. ➔ 7 cases**
  - Signed strength, Bd, of the surrounding arcade magnetic field

Parametric flux emergence simulations

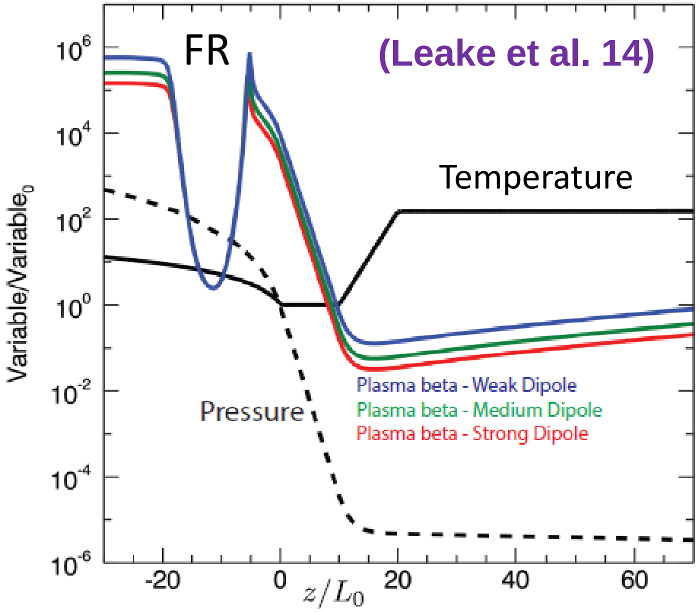

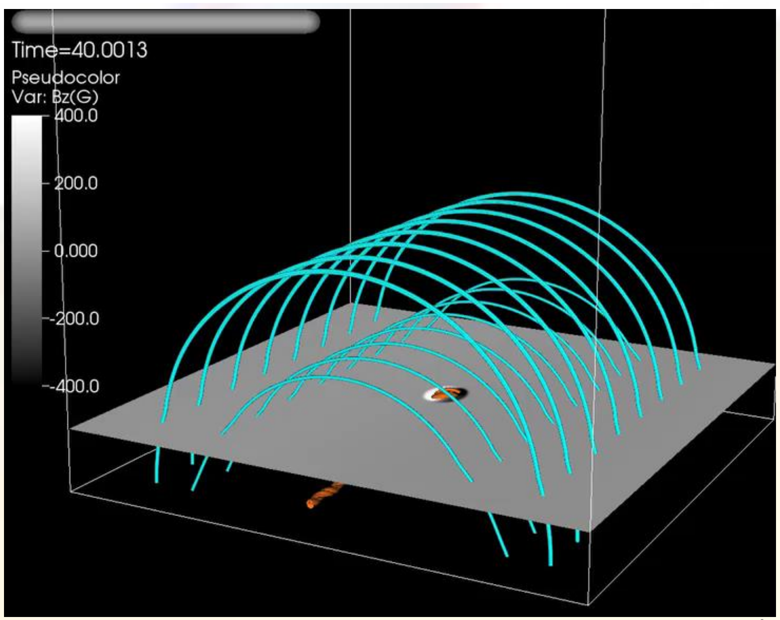

- Twisted FR emerge in coronal arcade field
- **Emerging twisted flux rope: identical in all cases**
- **Overlying arcade field: 1 param. ➔ 7 cases**
  - Signed strength, Bd, of the surrounding arcade magnetic field
  - Bd=0: no surrounding field
    - → stable flux rope in the corona
    - No eruption
  - Bd>0: same orientation of arcade field and azimuthal part of emerging field: interaction of // fields
    - → formation of stable flux rope
    - No eruption

Parametric flux emergence simulations

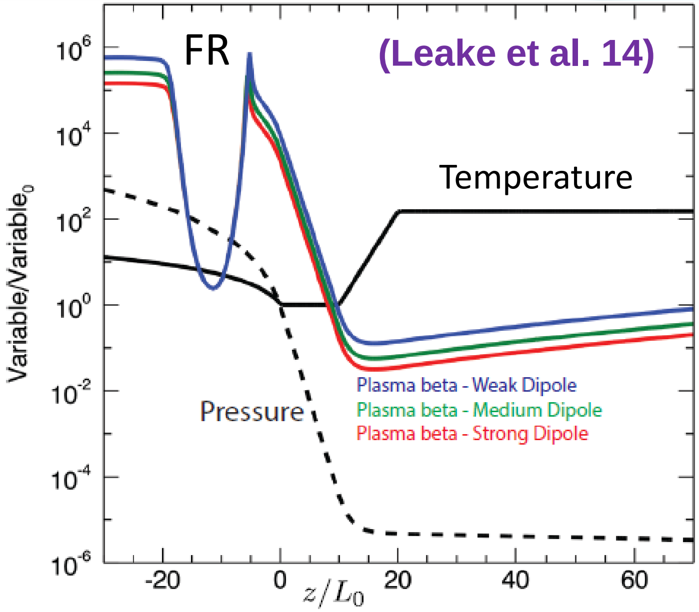

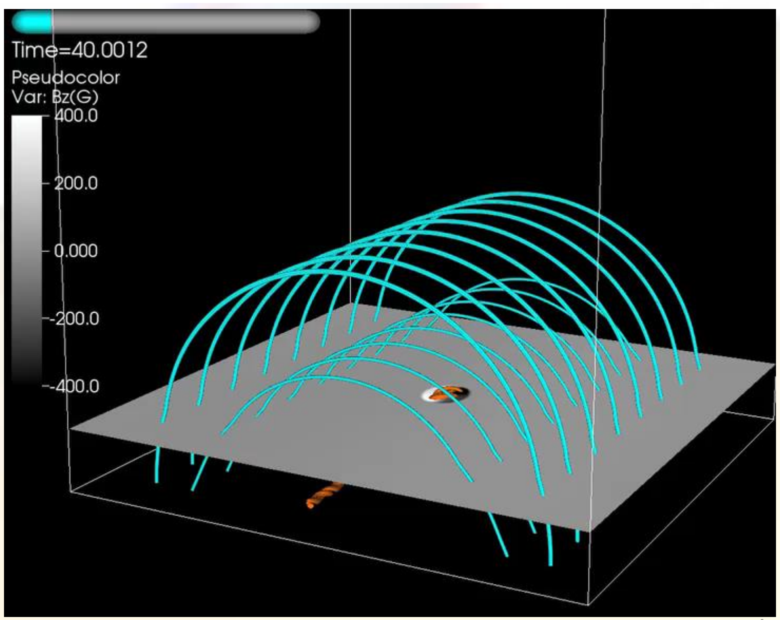

- Twisted FR emerge in coronal arcade field
- **Emerging twisted flux rope: identical in all cases**
- **Overlying arcade field: 1 param. ➔ 7 cases**
  - Signed strength, Bd, of the surrounding arcade magnetic field
  - Bd=0: no surrounding field
    - → stable flux rope in the corona
    - No eruption
  - Bd>0: same orientation of arcade field and azimuthal part of emerging field: interaction of // fields
    - → formation of stable flux rope
    - No eruption
  - Bd<0: opposite orientation of arcade field and azimuthal part of emerging field: interaction of anti-// fields
    - → reconnection and formation of unstable flux rope
    - Eruptive behavior

Search for eruptivity criterion

- **Emerging twisted flux rope: identical in all cases**
- **Overlying arcade field: 1 parameter ➔ 7 cases**

Label	No Erupt SD	No Erupt MD	No Erupt WD	No Erupt ND	Erupt WD	Erupt MD	Erupt SD
B_d	10	7.5	5	0	−5	−7.5	−10
Dipole Strength	Strong	Medium	Weak	Null	Weak	Medium	Strong
Eruption	No	No	No	No	Yes	Yes	Yes

- Eruptive simulations: onset at t ~ 120 t_0
- Non-eruptive simulation stable > 400 t_0

- **Goal: search for eruptivity indicators from 3D coronal magnetic datacube**
- Good eruptivity criterion should:
  - Discriminate eruptive and non-eruptive sim. during pre-eruptive phase
  - Reach its highest value
    - for eruptive simulation only,
    - during the pre-eruptive phase only.
  - Present similar trend for eruptive and non-eruptive sim. in post-eruptive phase

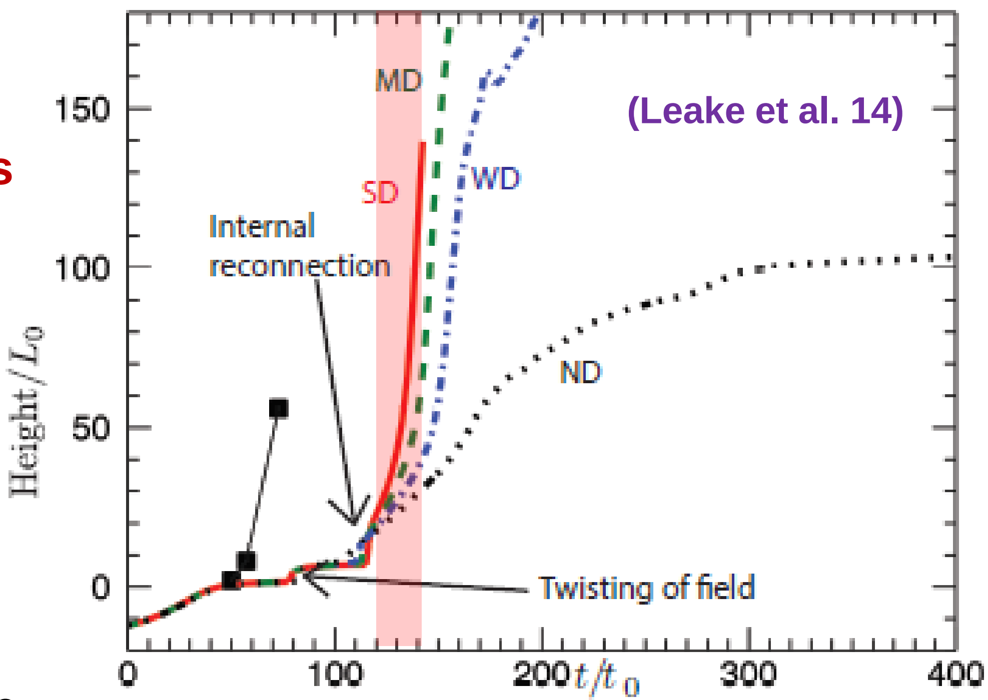

Outline

- Introduction: flare & eruption previsions
- Flux emergence model: Leake et al. 2013 & 2014
- **Eruptivity criterion analysis**
  - **Magnetic flux & energy-based quantities**
  - Magnetic-helicity-based quantities
    - Relative magnetic helicity
    - Current-carrying magnetic helicity
- Other models
- Conclusions

Magnetic fluxes

(Pariat et al. 17)

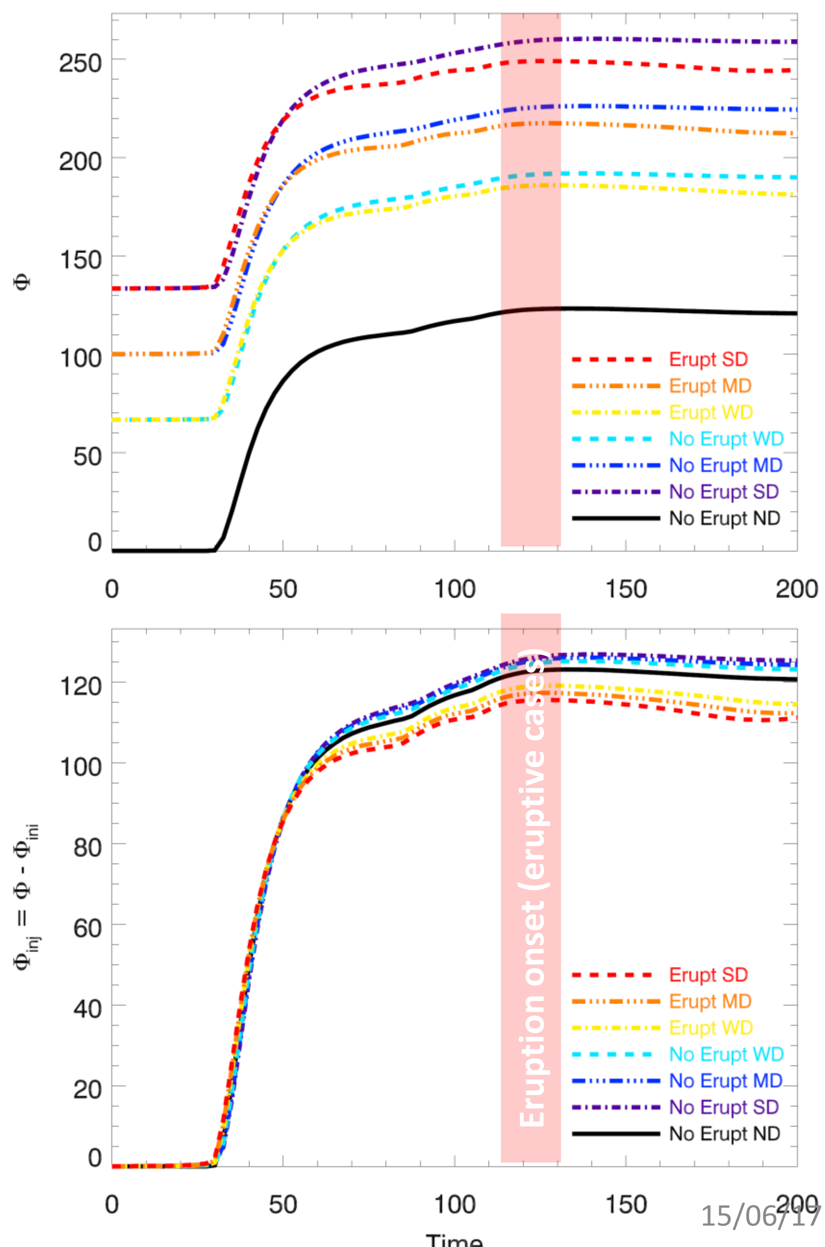

- Reference magnetic flux depends on the arcade field strength
- **Injected flux by emerging flux rope is roughly identical for all 7 simulations**

Magnetic fluxes

(Pariat et al. 17)

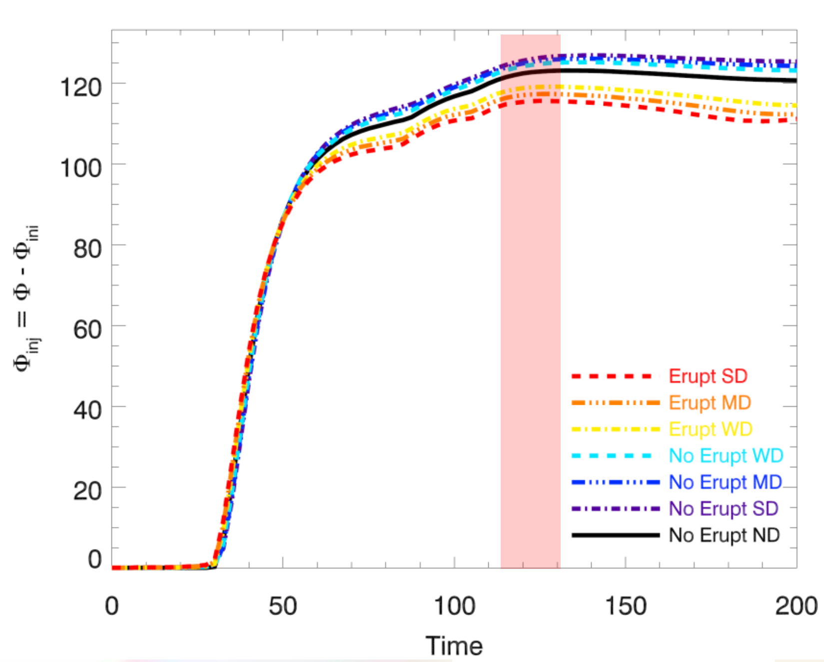

- Reference magnetic flux depends on the arcade field strength
- **Injected flux by emerging flux rope is roughly identical for all 7 simulations**

(Labonté et al. 07)

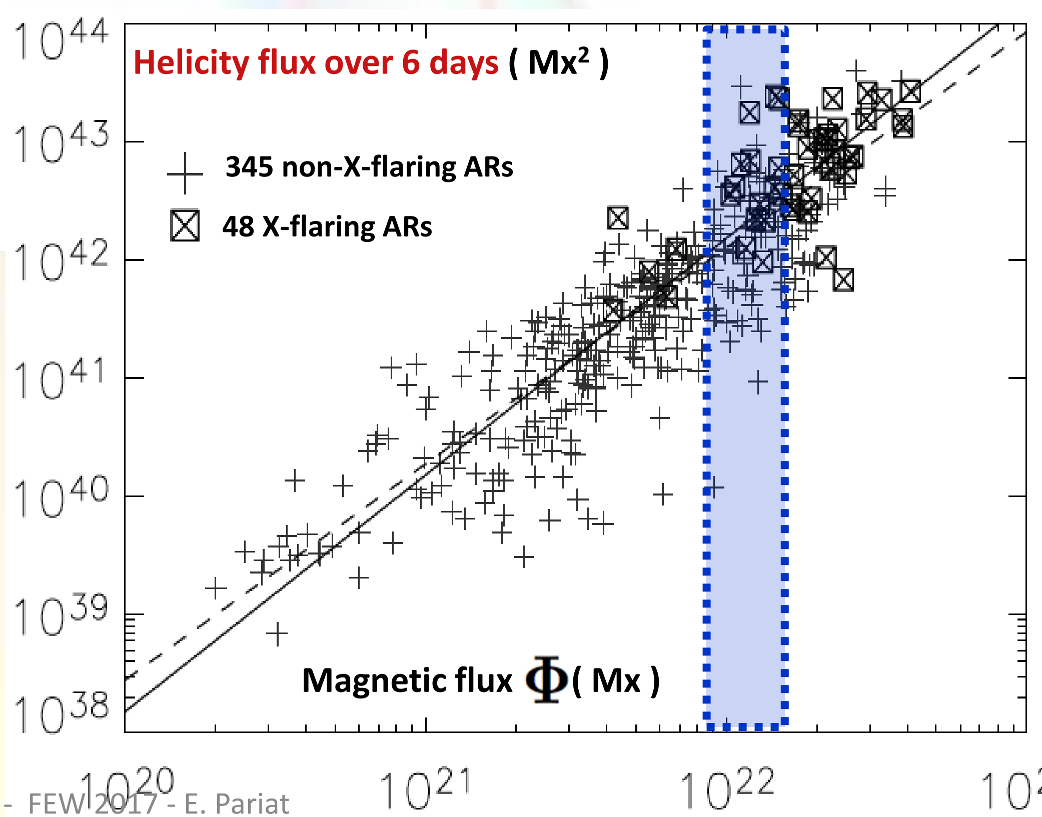

- Limits of the model: eruptivity criterion valid given a roughly constant injected magnetic flux.
- **➔ determining why active regions with a given magnetic flux erupt and others do not.**

Total and potential magnetic energy

$$E_{mag} = E_{pot} + E_{free} + E_{ns}\,,$$

- Eruptive simulation have a lower injection of total magnetic energy and potential magnetic energy.
- **Both total and potential magnetic energies are not good indictors of the eruptivity of the system**

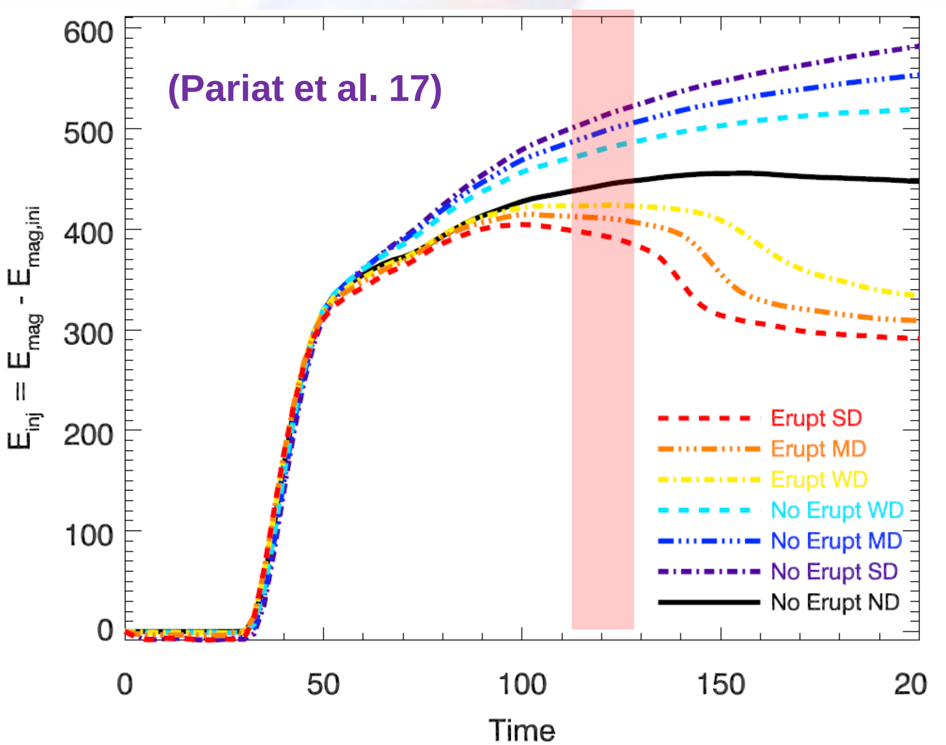

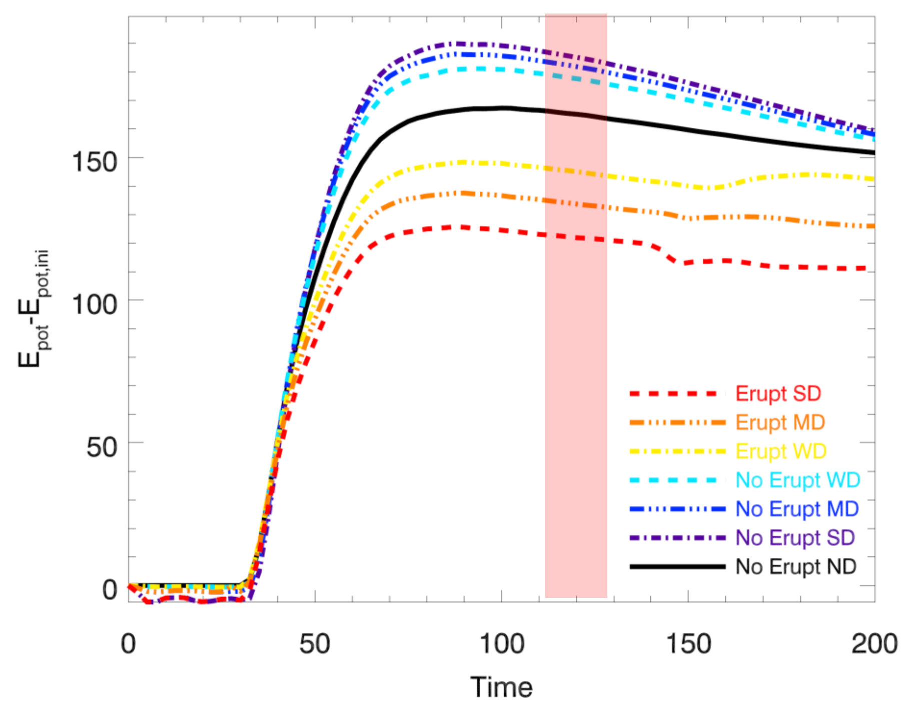

Free magnetic energy

$$E_{mag} = E_{pot} + E_{free} + E_{ns}$$

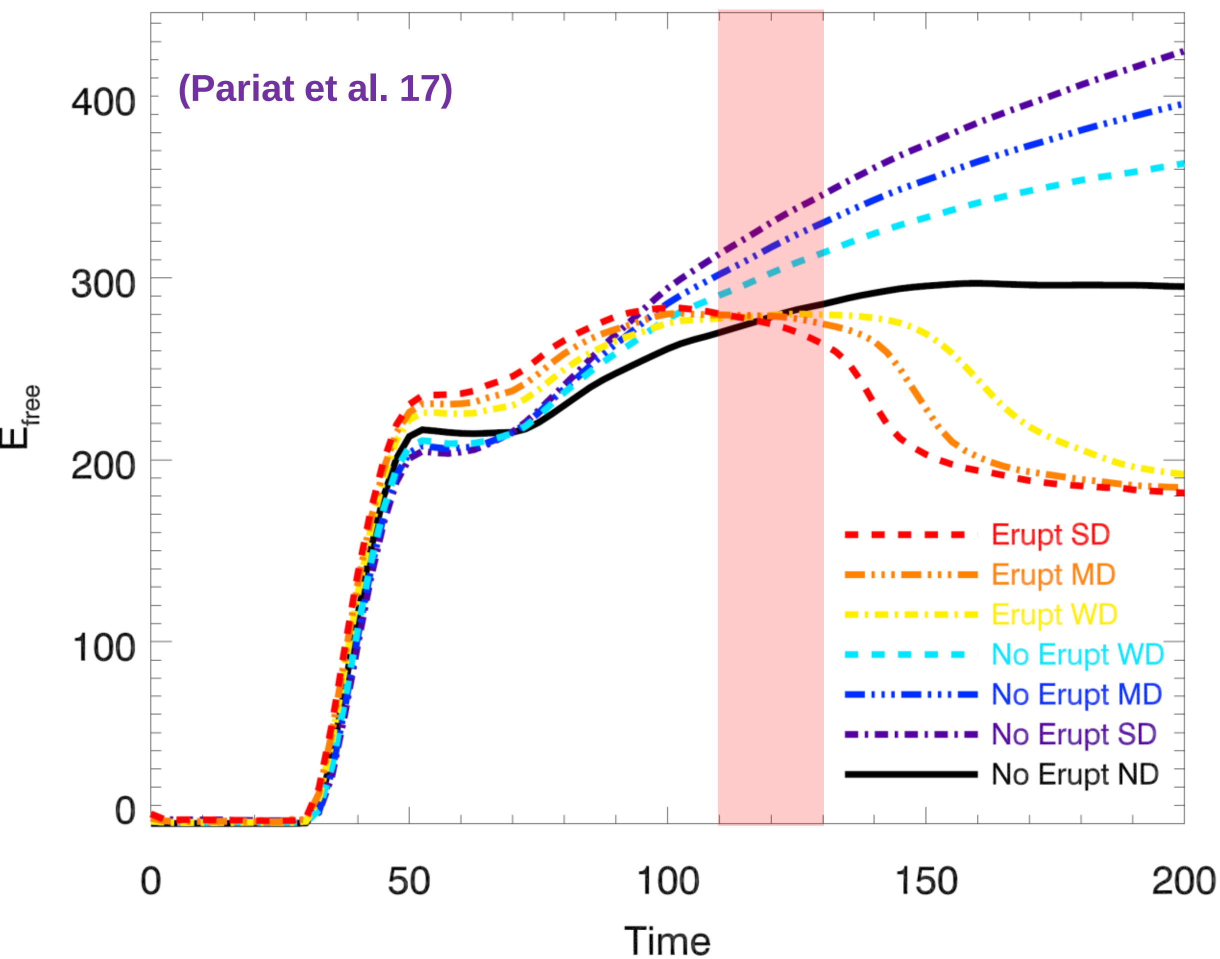

- Free energy is slightly higher for eruptive simulation in the pre-eruption phase.
- However highest value of E_{free} are reached by non-eruptive simulations.
- **Free magnetic energy is not a good indicator of the eruptivity state of the system**

Free magnetic energy ratio

$$E_{mag} = E_{pot} + E_{free} + E_{ns}$$

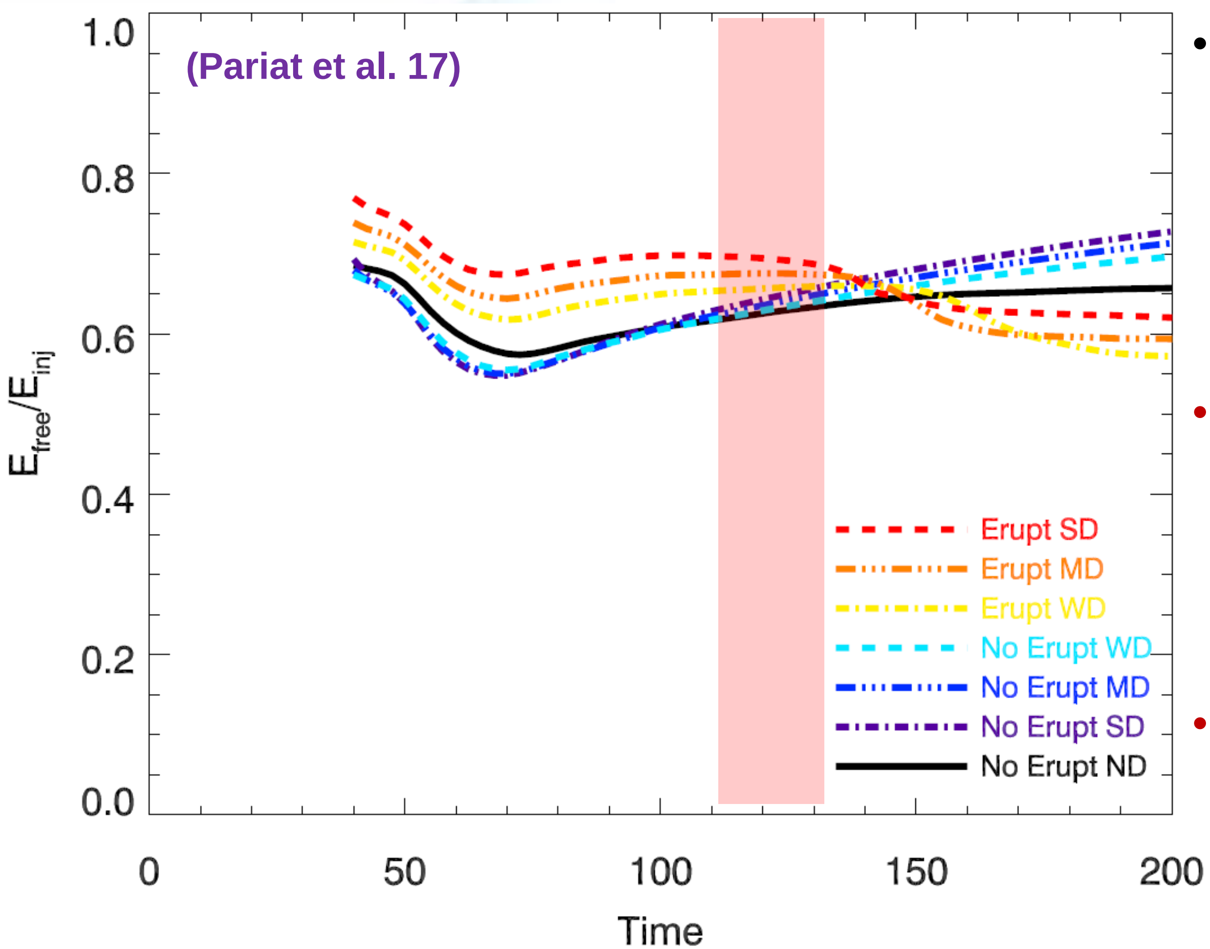

- E_{free}/E_{inj} is higher for eruptive simulation vs. non eruptive in the pre-eruption phase with marginally the highest values
- **Ratio of free magnetic energy to injected energy may be a proxy of eruptivity of the system**
- **However, E_{free}/E_{inj} not strongly discriminative: maximum value for eruptive flare are only marginally above non-eruptive ones.**

Outline

- Introduction: flare & eruption previsions
- Flux emergence model: Leake et al. 2013 & 2014
- **Eruptivity criterion analysis**
  - Magnetic flux & energy-based quantities
  - **Magnetic-helicity-based quantities**
    - **Relative magnetic helicity**
    - Current-carrying magnetic helicity
- Other models & Conclusions

Relative magnetic helicity

- **Magnetic helicity of MHD plasmas** **(Elsasser 1956)**

$$H = \int_{\mathcal{V}} \mathbf{A} \cdot \mathbf{B}\, \mathrm{d}\mathcal{V}$$

  - **unique signed scalar** value for volume considered
  - magnetic flux weighted Gauss Linking Number of pairs of magnetic field lines **(Moffatt 1968)** : signed level of entanglement & twist of field lines

- **Useful quantity for natural plasmas: Relative Magnetic Helicity**: helicity of a studied field relative to a reference field **(Berger 1984, Finn & Antonsen 1985).**

$$H_{\mathcal{V}} = \int_{\mathcal{V}} (\mathbf{A} + \mathbf{A}_{\mathrm{p}}) \cdot (\mathbf{B} - \mathbf{B}_{\mathrm{p}})\ \mathrm{d}\mathcal{V}$$

with boundary condition : $(\mathbf{B}_{\mathrm{p}} \cdot \mathrm{d}\mathbf{S})\,|_{\partial\mathcal{V}} = (\mathbf{B} \cdot \mathrm{d}\mathbf{S})\,|_{\partial\mathcal{V}}$

- Gauge invariant provided that studied and reference fields share the same magnetic-flux distribution on the <u>whole boundary</u>.

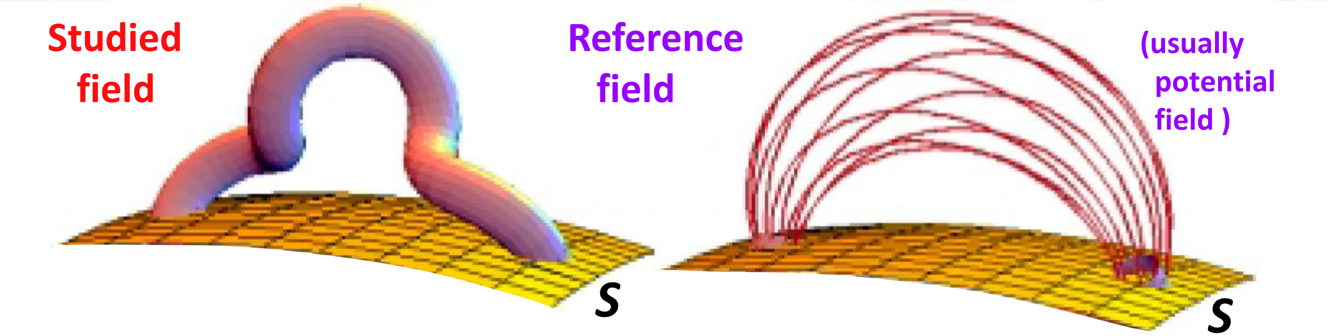

Magnetic helicity properties

- **Magnetic helicity is an ideal MHD invariant. For E⊥B: no dissipation ➔ magnetic helicity is conserved** **(Woltjer 1958).**

Time variations **Surface Flux** **Dissipation**

$$\frac{dH_m}{dt} = \int_{\partial\mathcal{V}} \left(\mathbf{A} \times \frac{\partial \mathbf{A}}{\partial t}\right) \cdot \mathrm{d}\mathbf{S} - 2\int_{\partial\mathcal{V}} (\mathbf{E} \times \mathbf{A}) \cdot \mathrm{d}\mathbf{S} - 2\int_{\mathcal{V}} \mathbf{E} \cdot \mathbf{B} \;\; \mathrm{d}\mathcal{V}$$

- **Taylor 1974: hypothesis helicity conservation true even in non-ideal MHD**
  - **Pariat et al. 16 : verified for a solar like active event**

- Magnetic helicity bounds the system E distribution:

$$\mu_0 \hat{E}(k) > k\hat{H}(k)$$ **(Frisch et al. 1975)**

- **Inverse helicity cascade:** Helicity goes from small to large spatial scales. **(Frisch et al. 1975, Alexakis et al. 2006)**
  - e.g. kink instability **(Malanushenko et al. 2009)**

- Impact on dynamic of magnetic reconnection: **e.g. Linton et al. 2001, Del Soro et al. 2010**

(Török et al. 05)

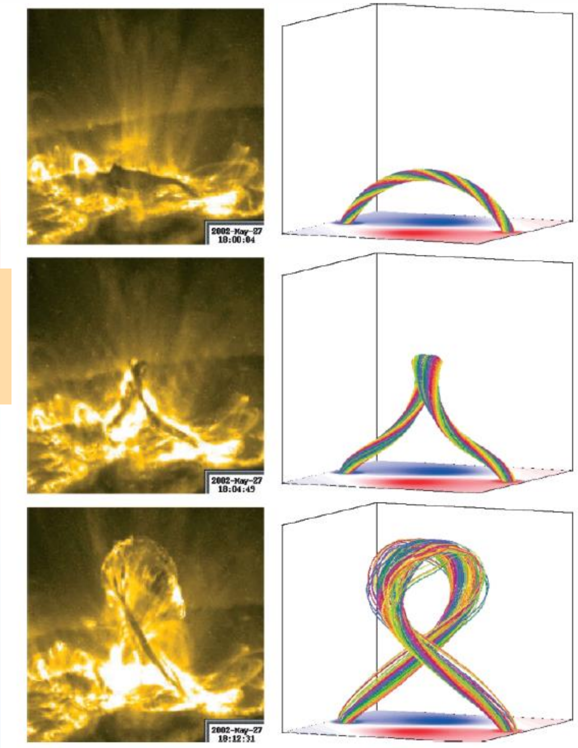

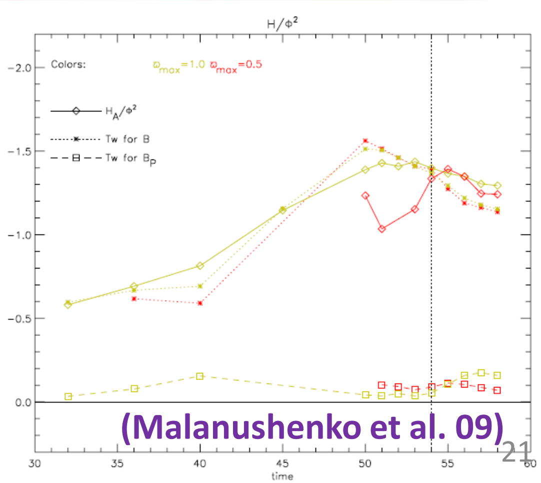

(Malanushenko et al. 09)

Relative Magnetic Helicity Estimations

- The computation of relative magnetic helicity is not straightforward:
  - **Computation of reference field must be done imposing boundary conditions on the whole domain boundary.**
  - Many previous methods assumed semi-infinite volumes while all existing datasets are bounded volumes: could lead to incorrect results **(Valori et al. 2011, 2012)**, error in intensity, even in sign!

- **Several methods recently developed on 3D cuboid system** **(Valori et al. 2016)**
  - Using Coulomb gauge: $\nabla \cdot \mathbf{A} = 0$

    Thalmann et al. 2011, **Rudenko & Myshyakov 2011, Yang et al. 2013**
    - Simpler theoretical formulation
    - Harder to implement numerically
  - Using DeVore gauge **(DeVore et al. 2000)** : $A_z = 0$

    Valori, Démoulin & Pariat 2012, Moraitis et al. 2014
    - More complex theoretical formulation
    - Simpler to implement numerically: more precise
- **New method to compute relative magnetic helicity in spherical wedge domains**. **(Moraitis et al. in prep.)**

Relative magnetic helicity estimations

- **Benchmarking of these methods performed by ISSI team on "Helicity estimations in models and observations“**: **Valori et al. 2016**
- Numerous tests: sensibility to resolution, twist, solenoidality using various types of data.
  - Force free fields **(Low & Lou 1990)**
  - Stable flux rope (**Titov & Démoulin 1999**, data fromT. Török)
  - Flux emergence simulations **(Leake et al. 2013, 2014)**
- **Methods perform very consistently when B sufficiently solenoidal**

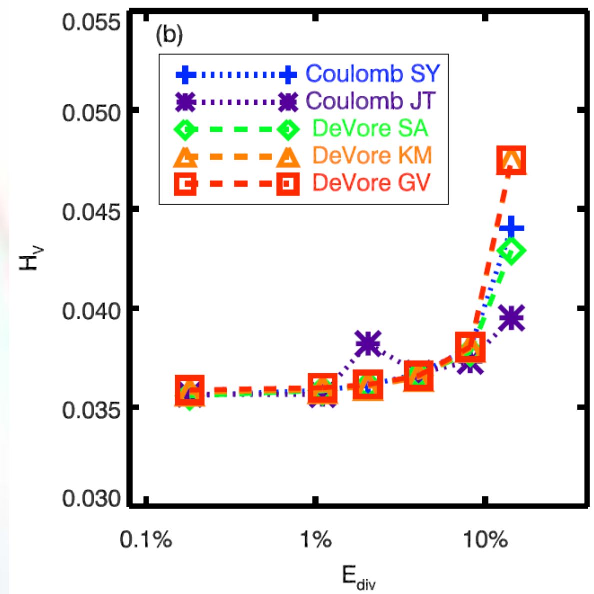

(Valori et al. 16)

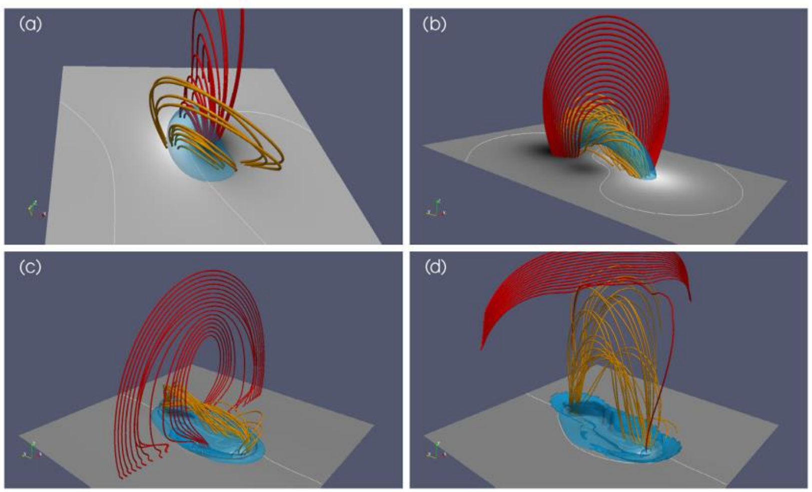

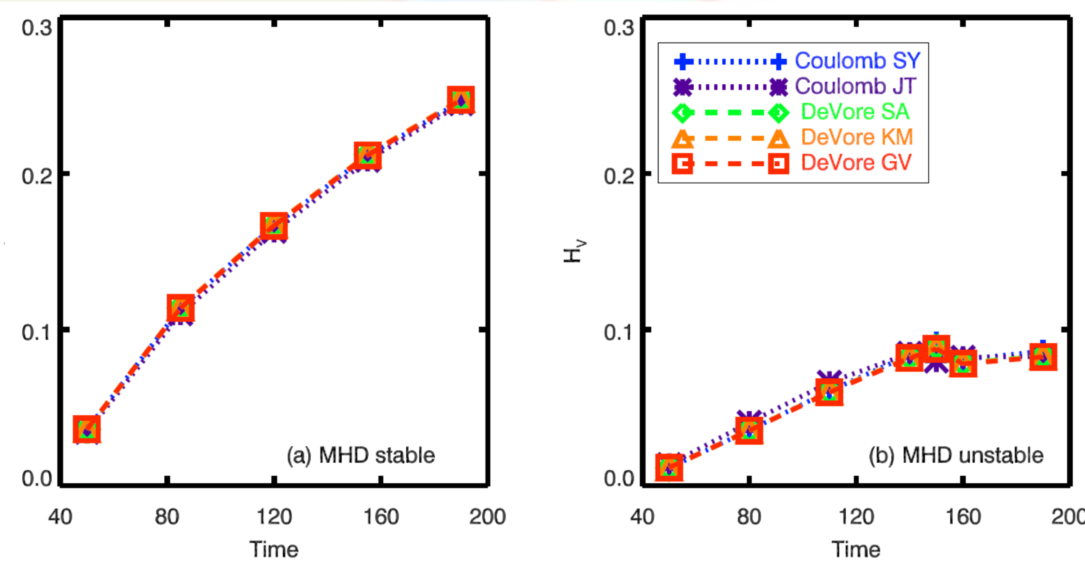

Relative magnetic helicity evolution

(Pariat et al. 17)

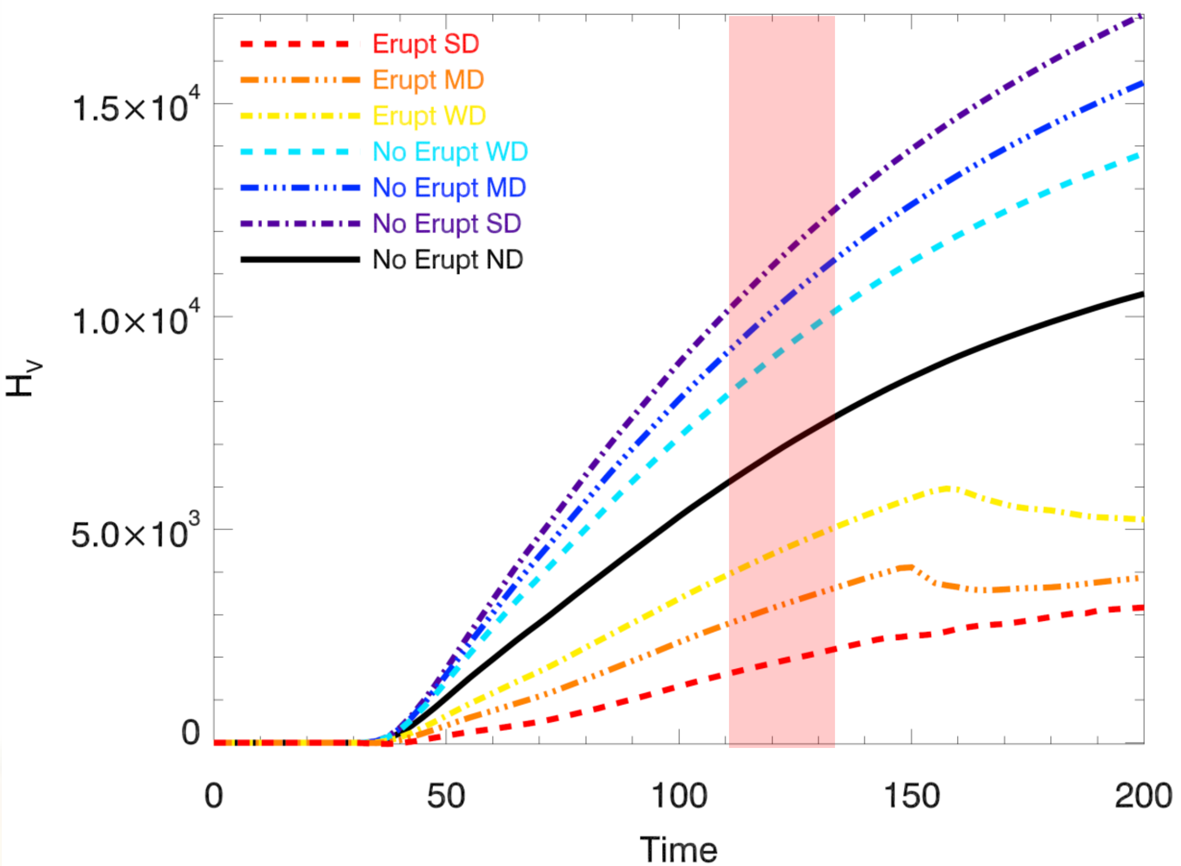

- **Unlike with magnetic flux & free energy, helicity discriminates strongly the cases**
  - Total helicity depends
    - on dipole strength
    - on dipole orientation

- The surrounding (potential) field influences the helicity content!
- **Magnetic helicity is a non-local quantity!**

- **Unlike what is commonly believed/expected, large total helicity is not a sufficient condition of eruptivity.**

Outline

- Introduction: flare & eruption previsions
- Flux emergence model: Leake et al. 2013 & 2014
- **Eruptivity criterion analysis**
  - Magnetic flux & energy-based quantities
  - **Magnetic-helicity-based quantities**
    - Relative magnetic helicity
    - **Current-carrying magnetic helicity**
- Other models & Conclusions

Relative magnetic helicity decomposition

$$
\begin{aligned}
H_V &= H_{\mathrm{j}} + 2H_{\mathrm{pj}} \quad \text{with} \\
H_{\mathrm{j}} &= \int_{\mathcal{V}} (\mathbf{A} - \mathbf{A}_{\mathrm{p}}) \cdot (\mathbf{B} - \mathbf{B}_{\mathrm{p}})\, \mathrm{d}\mathcal{V} \\
H_{\mathrm{pj}} &= \int_{\mathcal{V}} \mathbf{A}_{\mathrm{p}} \cdot (\mathbf{B} - \mathbf{B}_{\mathrm{p}})\, \mathrm{d}\mathcal{V}
\end{aligned}
$$

- **Berger et al. 2003 :** relative magnetic helicity can be decomposed in 2 quantities:
  - H_j = magnetic helicity of the current-carrying/non-potential field B_j
  - H_{pj} = intra-helicity between potential and current carrying fields
- H_V, $H_{j,}$ & H_{pj} are all gauge invariant.
- Remark for the heli-aware: $H_{j,}$ & H_{pj} are different from the “self” and “mutual” helicities

Helicity decomposition evolution

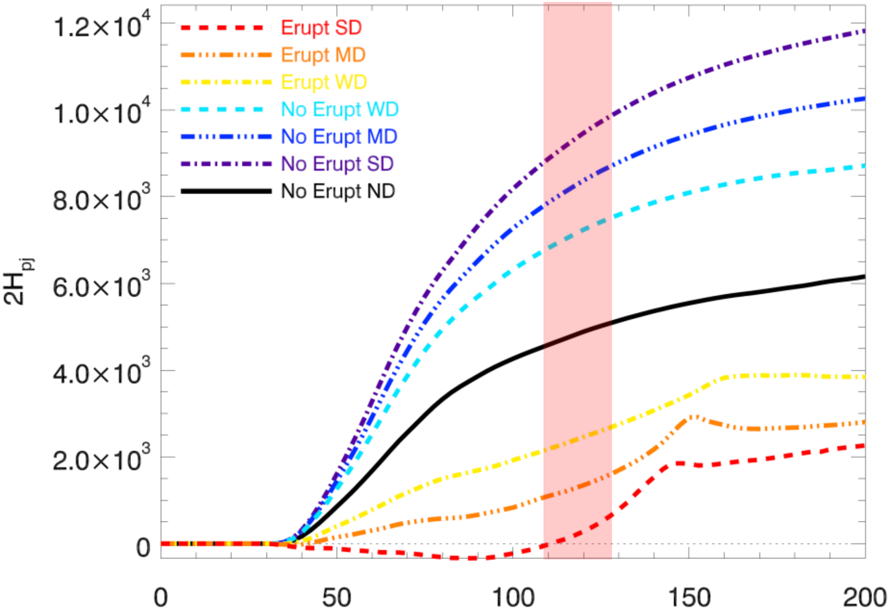

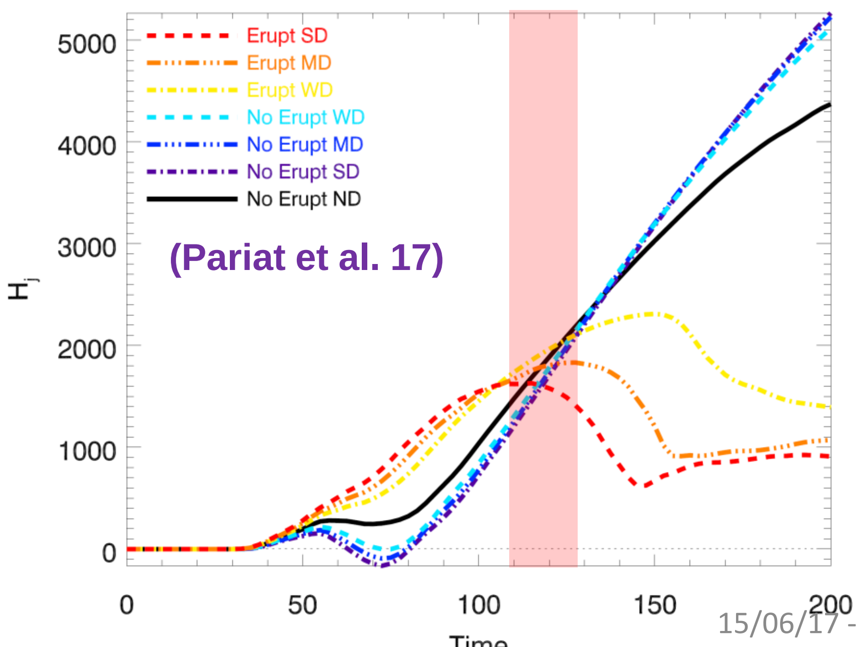

$$
\begin{aligned}
H_{\mathcal{V}} &= H_{\mathrm{j}} + 2H_{\mathrm{pj}} \quad \text{with} \\
H_{\mathrm{j}} &= \int_{\mathcal{V}} (\mathbf{A} - \mathbf{A}_{\mathrm{p}}) \cdot (\mathbf{B} - \mathbf{B}_{\mathrm{p}})\, \mathrm{d}\mathcal{V} \\
H_{\mathrm{pj}} &= \int_{\mathcal{V}} \mathbf{A}_{\mathrm{p}} \cdot (\mathbf{B} - \mathbf{B}_{\mathrm{p}})\, \mathrm{d}\mathcal{V}
\end{aligned}
$$

- Total helicity is overall dominated by $2H_{pj}$
- $2H_{pj}$ has same properties than total helicity ➔ not a good eruptivity proxy
- **H_j behaves similarly to E_{free}**
  - **higher for the eruptive simulations in the pre-eruptive phase**
  - **however higest values reached by non-eruptive simulations**
- **H_j is not a good eruptivity proxy.**

$|H_j|/|H_V|$: excellent eruptivity indicators

(Pariat et al. 17)

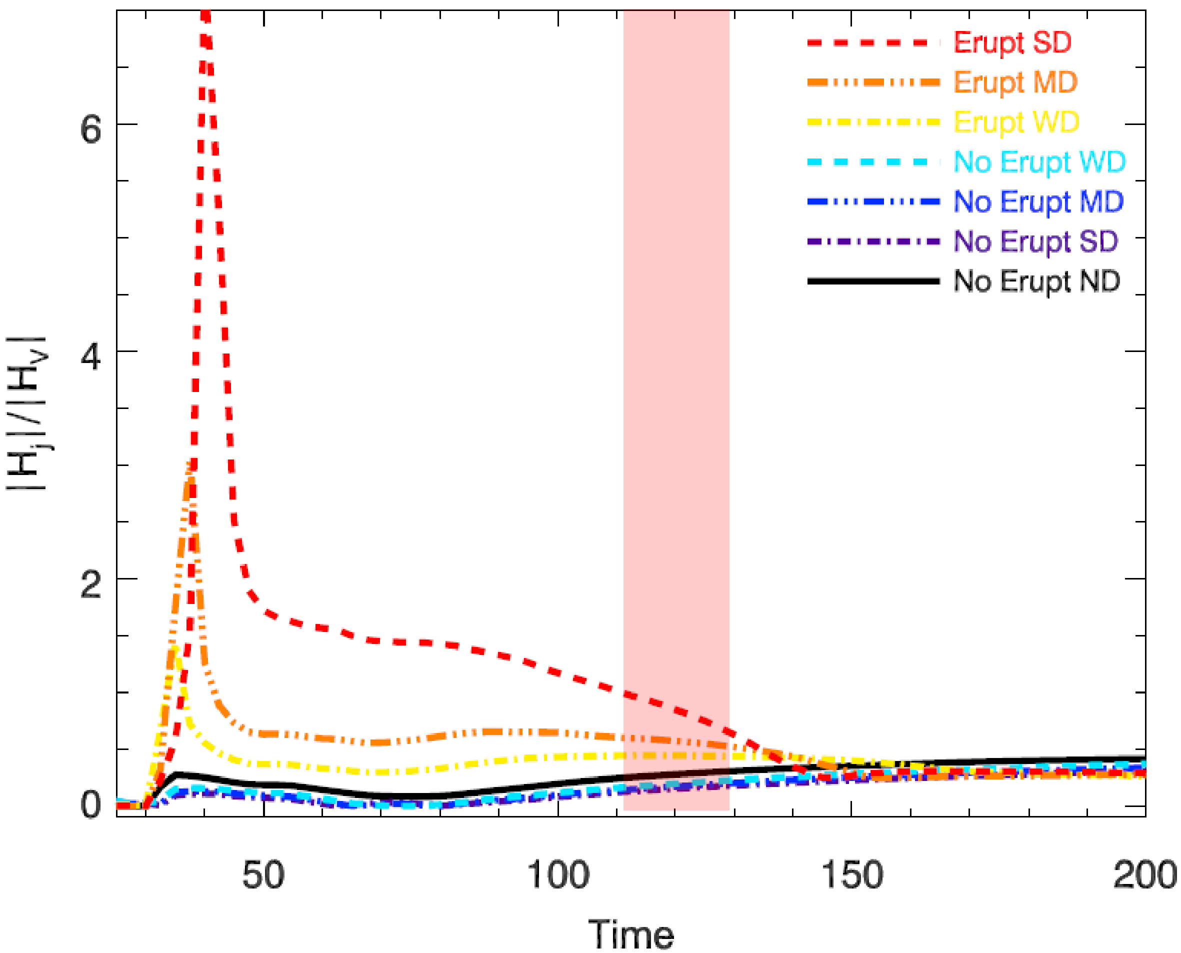

$$
\begin{aligned}
H_V &= H_j + 2H_{pj} \quad \text{with} \\
H_j &= \int_{\mathcal{V}} (\mathbf{A} - \mathbf{A}_p) \cdot (\mathbf{B} - \mathbf{B}_p)\, d\mathcal{V} \\
H_{pj} &= \int_{\mathcal{V}} \mathbf{A}_p \cdot (\mathbf{B} - \mathbf{B}_p)\, d\mathcal{V}
\end{aligned}
$$

- **$|H_j|/|H_V|$ appears as an excellent eruptivity predictor of these sims.**
  - **Highest value for the eruptive simulations in the pre-eruptive phase**
  - **Eruptive and non-eruptive simulations have similar values in post-eruption phase**

- $|H_j|/|H_V|$ is also sensitive to dipole strength which fits with promptness to erupt

Outline

- Introduction: flare & eruption previsions
- Flux emergence model: Leake et al. 2013 & 2014
- Eruptivity criterion analysis
  - Magnetic flux & energy-based quantities
  - Magnetic-helicity-based quantities
    - Relative magnetic helicity
    - Current-carrying magnetic helicity
- **Other models & conclusions**

More evidences : other flux emerg. simulations

- **Moraitis et al. 2014**: analyze of the helicity content of 2 flux emergence simulations (not directly comparable) :
  - Non-eruptive **(e.g. Archontis et al. 2004)**
  - Multi-eruptive **(e.g Archontis et al. 2014)**

(Moraitis et al. 14)

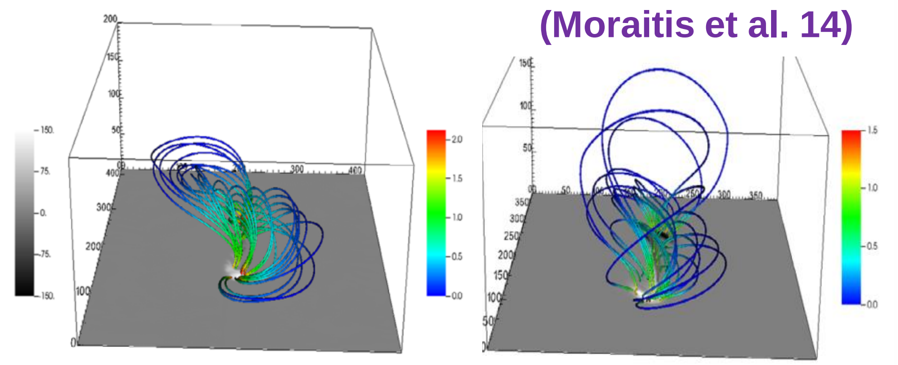

- **Multi-eruptive case:**
  - **Systematic high values of $|H_j|/|H_V|$ some time before the eruptions onset.**
  - $|H_j|/|H_V|$ decreases after eruptions

- **Non-eruptive case: constant and relatively lower values of $|H_j|/|H_V|$**

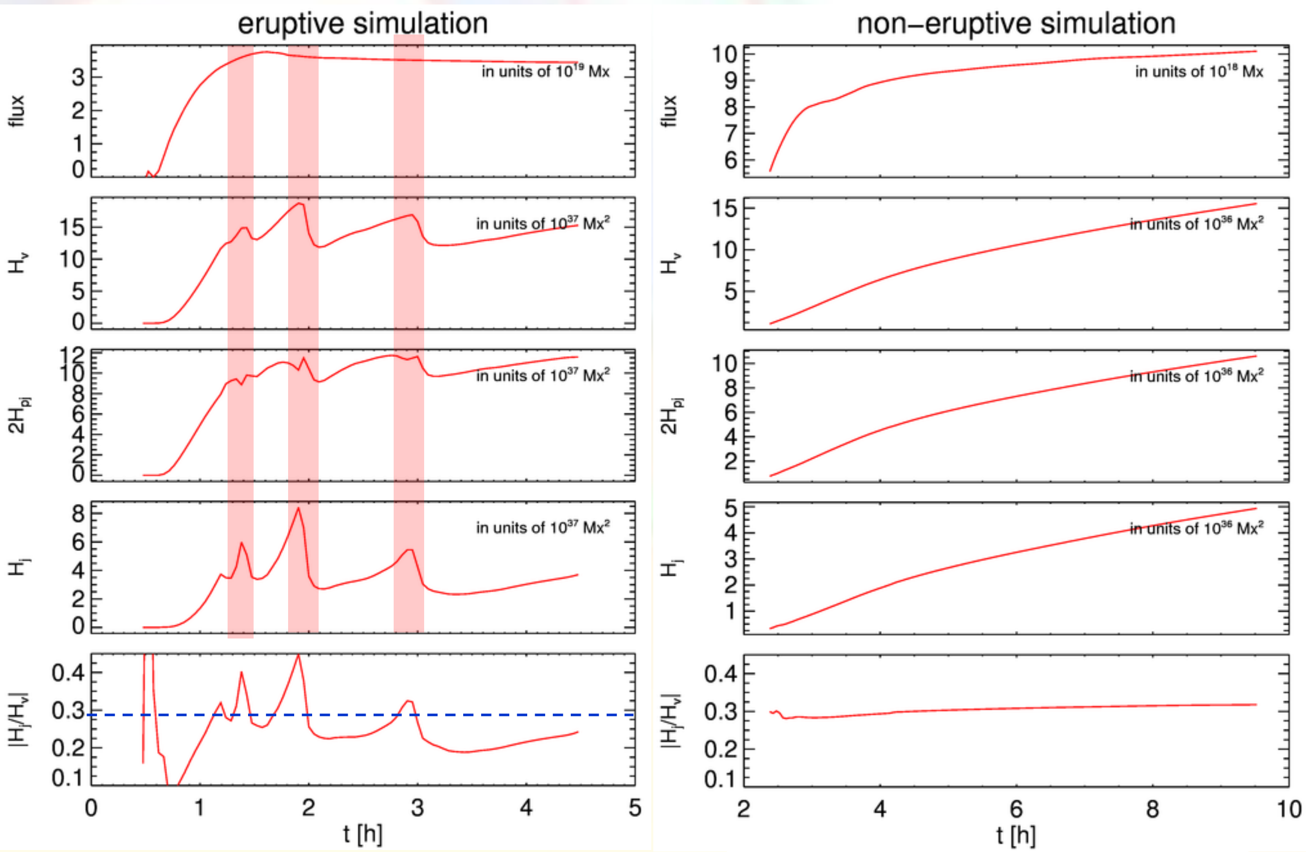

(Figure by K. Moraitis)

More evidences: jet simulation

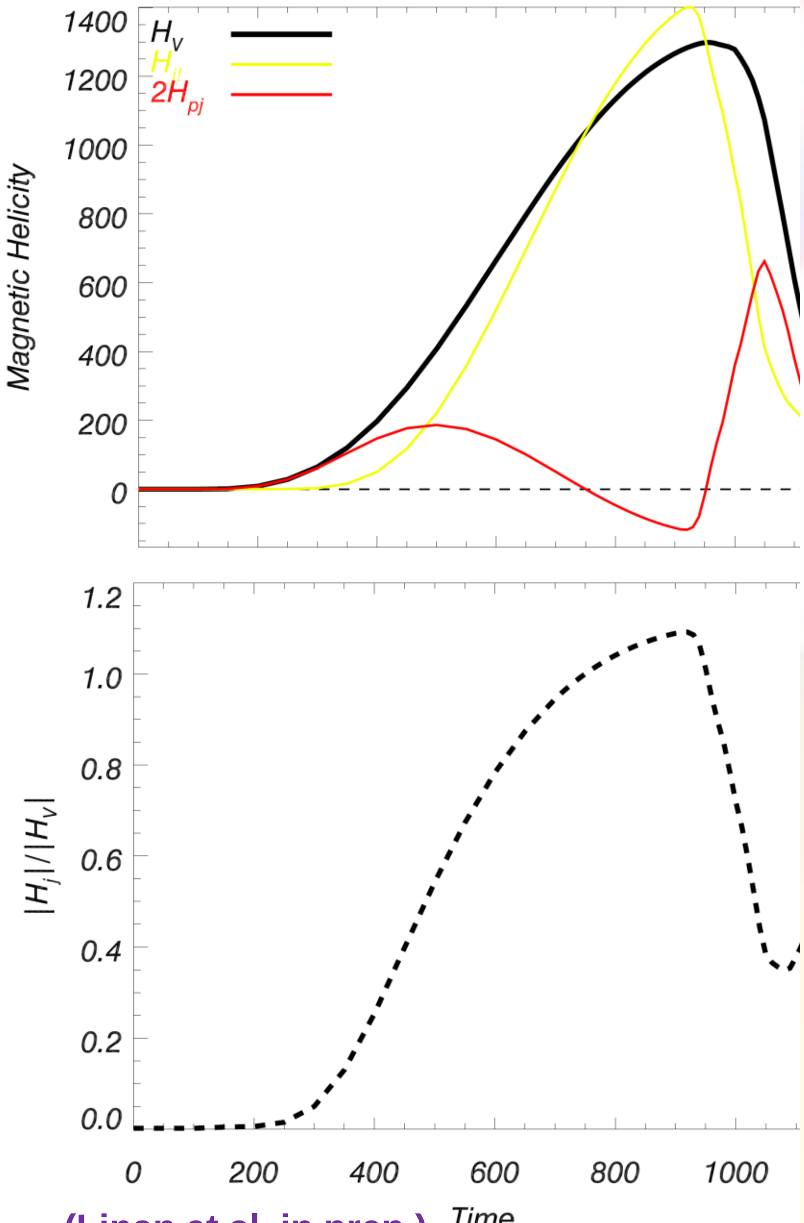

(Linan et al. in prep.)

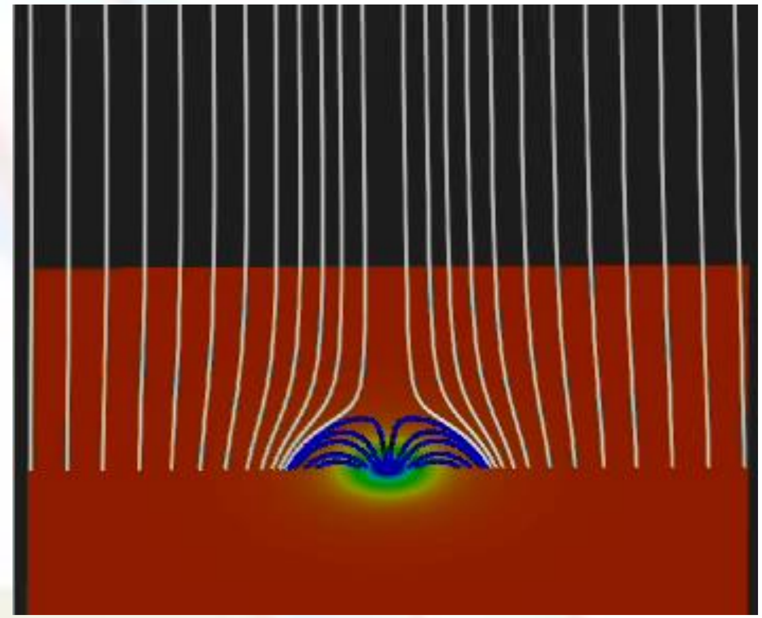

- Coronal jet simulations: **Pariat et al 09, 15**
- **Helicity initially dominated by H_{pj} but H_j become dominant after t~500**
- **Very high value of $|H_j|/|H_V|$ at jet onset.**
  - Remark: system “over” eruptive due to topological constraints
- $|H_j|/|H_V|$ returns to low value once the system has relaxed.

Further evidences : torus-instability triggered eruptive simulations

- **Zuccarello et al. 2015**: parametric eruptive simulations
- **4 different line-tied boundary driving patterns** with different: shear around the PIL magnetic flux dispersion + 1 non-eruptive control case (diffusion)
- **Precise determination of the onset time, t_{erupt}, thanks to numerous relaxation runs initiated at regular stage of the simulations**

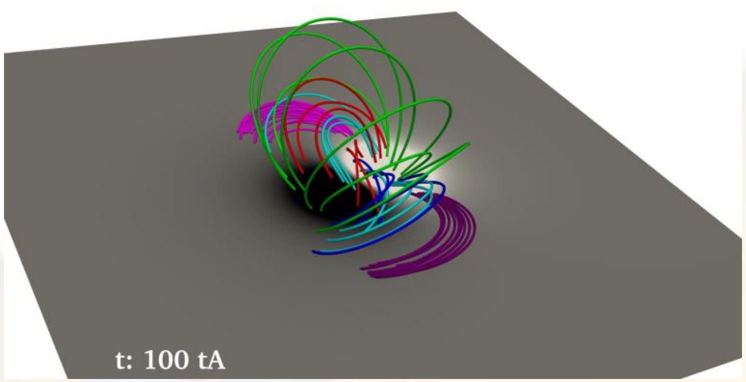

(Aulanier et al. 10, Zuccarello et al. 16)

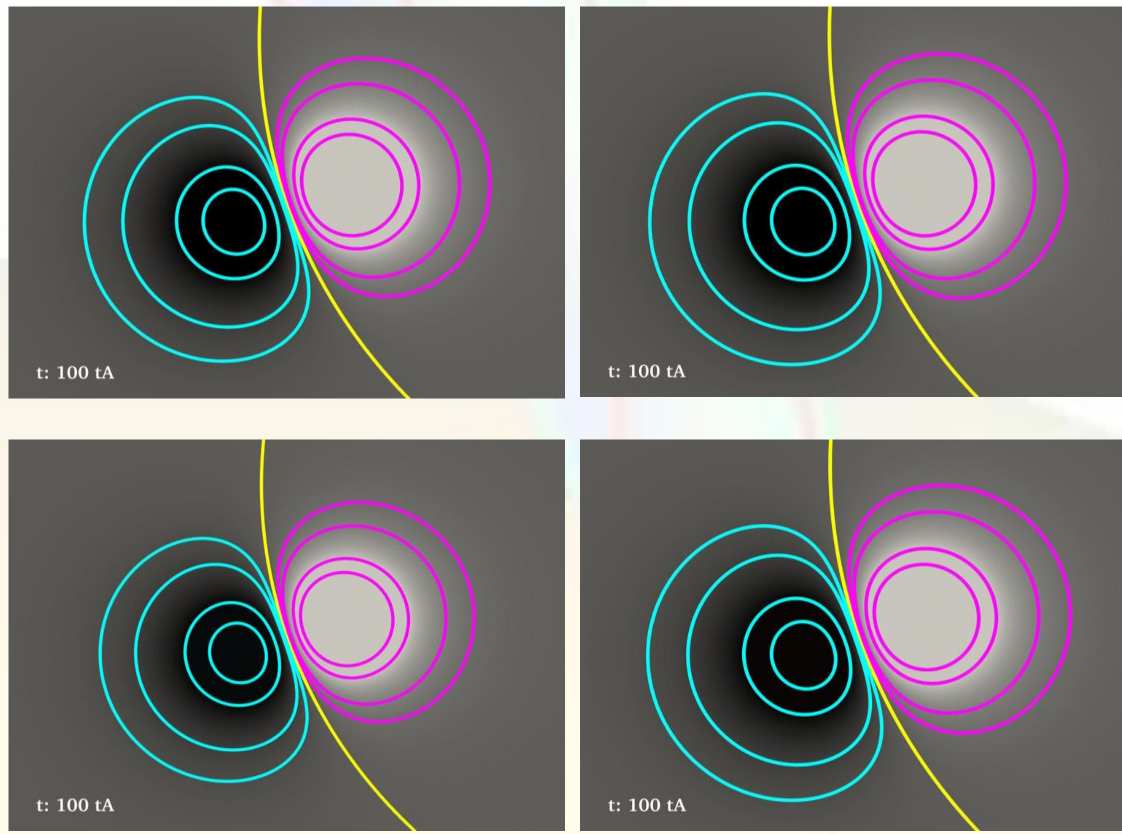

Further evidences : torus-instability triggered eruptive simulations

- Computation of several quantities at the sim. respective t_{erupt} : **Zuccarello et al. to be submitted.**

- **Despites different boundary drivers and t_{erupt}, eruptions are triggered when $|H_j|/|H_V|$ reaches the same value:**
  - <4% dispersion
  - within measurement precision of helicity

- All other quantities have dispertions of values above 8 % at t_{erupt} , including torus instability criteria

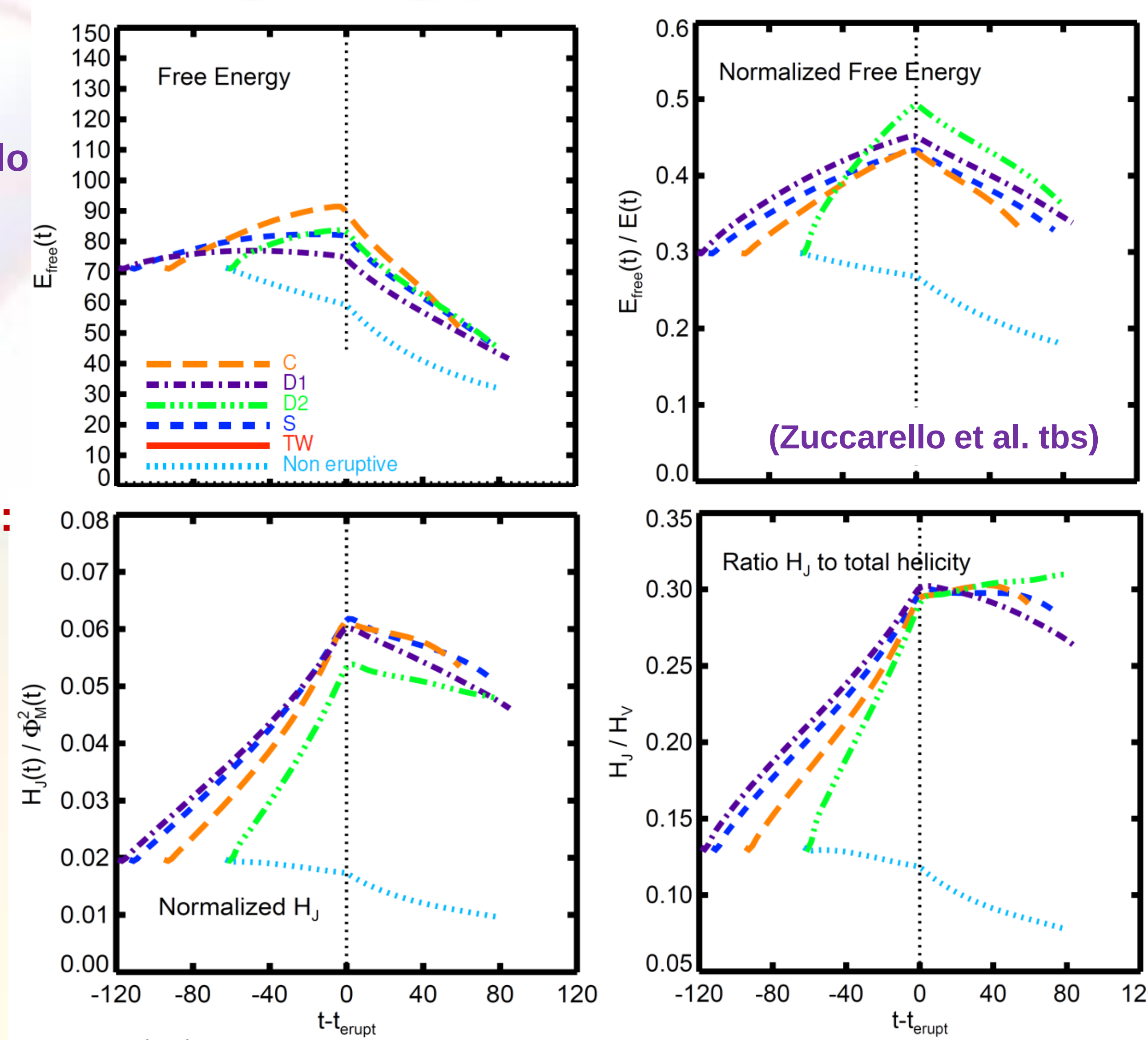

Conclusions

- (too) Rare attempts to use parametric numerical simulation to study eruptivity proxy of solar active events.
- Flux and energy-based quantities are poor discriminant and poor eruptivity. proxies in these models
- **Magnetic helicity based quantities allow to easily discriminate between the different parametric simulations**
- **The ratio |Hj|/|Hv| is an excellent indicator of the eruptivity state in several numerical models**
  - 4 different magnetic systems
  - 3 different MHD numerical codes

(Labonté et al. 07)

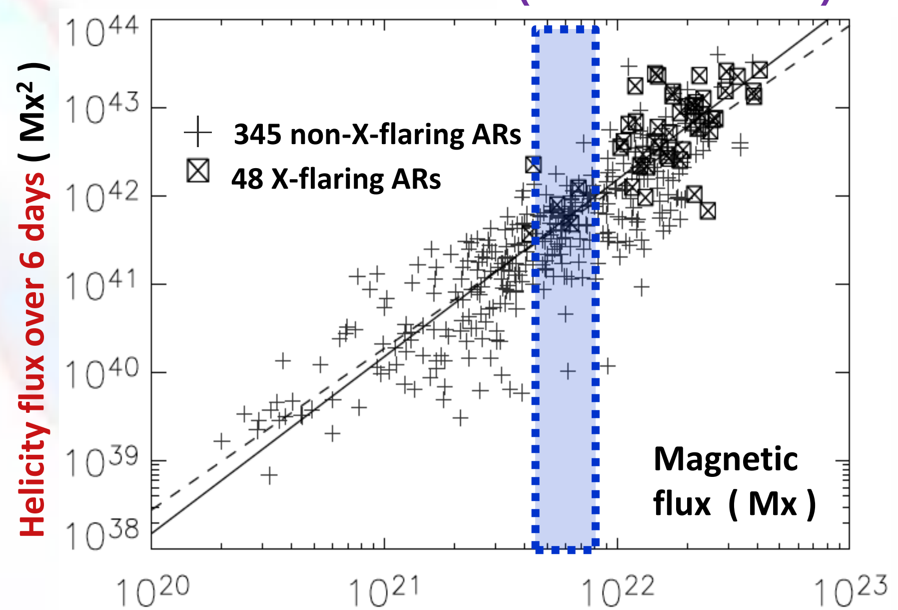

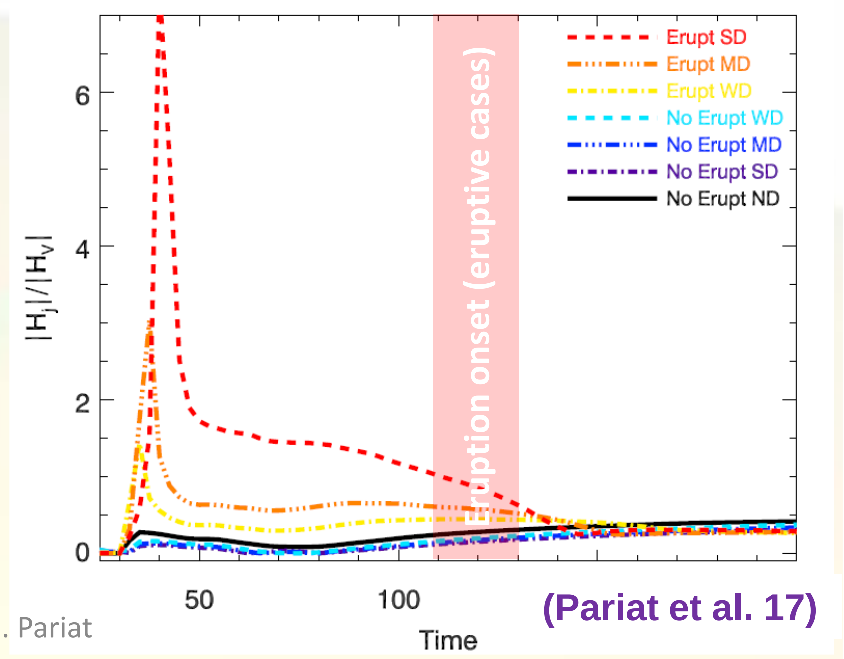

(Pariat et al. 17)


Thanks for your attention
I hope that this talk was worth a Havana

Relative magnetic helicity evolution

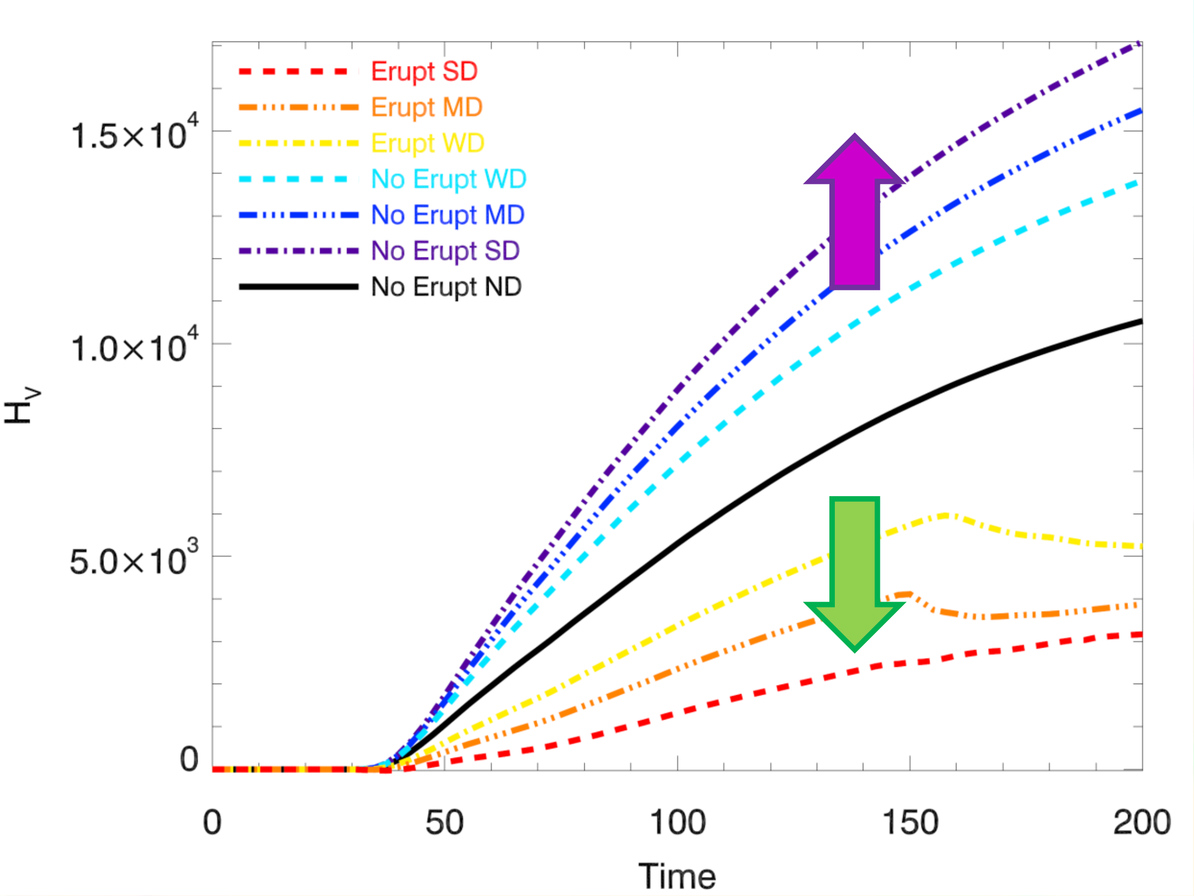

- Helicity of the stable cases is larger than the eruptive cases !
- Helicity **increases with arcade strength for non-eruptive cases**
- Helicity **decreases with arcade strength for eruptive cases**

Self and Mutual helicity

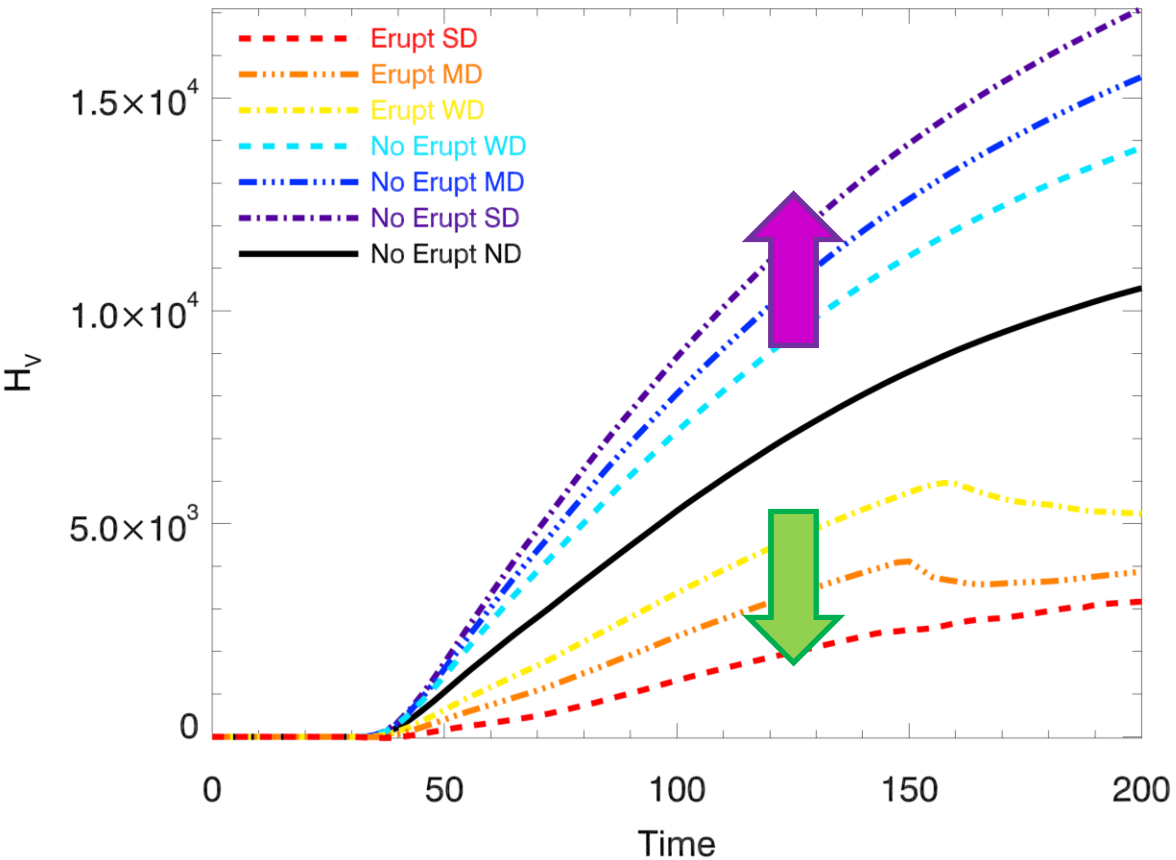

- Helicity decomposition in **self** and **mutual** helicity of flux rope and arcade

  $H = H_{self,fr} + H_{mutual} + H_{self,arc}$

- **$H_{self,fr}$** = H(No Erupt ND) $\alpha\ \Phi_{fr}^2$
- **$H_{self,arc}$** = 0
- **H_{mutual}** $\alpha\ \Phi_{fr}\ \Phi_{arc}$;
  - sign depends on relative orientation

- Non-eruptive cases: FR & arcade have same orientation : **$H = H_{self,fr} + |H_{mutual}|$**
- Eruptive cases: FR & arcade have opposite orientation: **$H = H_{self,fr} - |H_{mutual}|$**
- With increasing dipole strength **$|H_{mutual}|$** increases
  - Qualitatively & quantitative match
    - H **increases for stable cases**
    - H **decreases for unstable**

Self and Mutual helicity

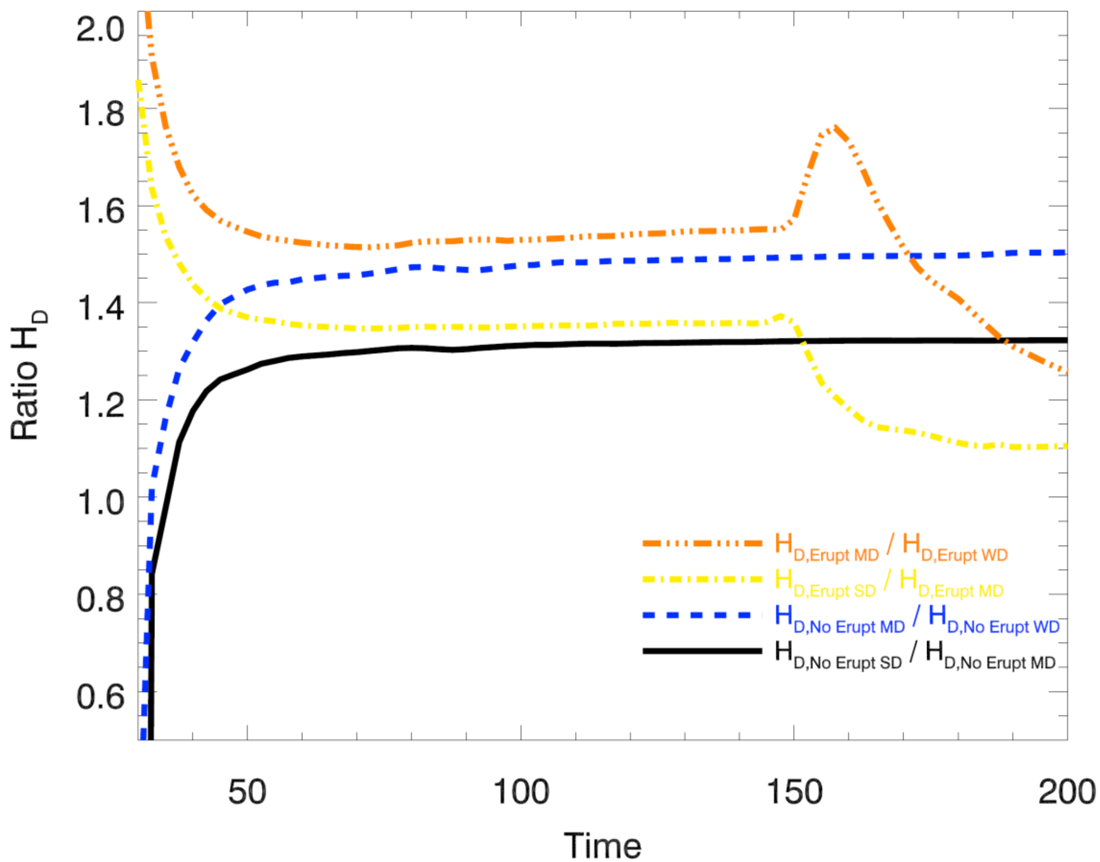

- Helicity decomposition in **self** and **mutual** helicity of flux rope and arcade

  $H = H_{self,fr} + H_{mutual} + H_{self,arc}$

- **$H_{self,fr}$** = H(No Erupt ND) $\alpha\ \Phi_{fr}^2$
- **$H_{self,arc}$** = 0
- **H_{mutual}** $\alpha\ \Phi_{fr}\ \Phi_{arc}$;
  - sign depends on relative orientation

- Very good quantitative match of this toy model
- Computation of HD: $H_D = H_V - H_{V,\,\text{No Erupt ND}} \sim \pm L\Phi_{Arc}$
- Toy model predict that ratio of HD shall be equal to magnetic flux ratios
- Good fit with expected values: $\Phi_{ini,\,MD}$ / $\Phi_{ini,WD}$ = 1.5 & $\Phi_{arcini,\,SD}$ / $\Phi_{ini,MD}$ = 1.33
- Problem: here self and mutual helicity can only be roughly estimated because we have a parametric dataset. Not the case with real data.